

**STATIC STIFFNESS ANALYSIS OF AN EMBEDDED BUCKET
FOUNDATION USING FINITE-ELEMENT MODELING**

A Thesis

By

YAMINI GROVER

Submitted to the Office of Graduate and Professional Studies of
Texas A&M University
in partial fulfillment of the requirements for the degree of
MASTER OF SCIENCE

Chair of Committee, Charles Aubeny
Committee Members, Marcelo Sanchez
Moo-Hyun Kim
Head of Department, Zachary Grasley

May 2023

Major Subject: Civil Engineering

Copyright 2023 Yamini Grover

ABSTRACT

Response of a rigid tube embedded in a homogeneous elastic-half space medium is the most fundamental yet important practice for evaluating the behavior of offshore wind turbine (OWT) foundations. A single degree of freedom (SDOF) spring-mass-dashpot system is deployed to characterize the interaction of a shallow foundation with underlying elastic-half space. The soil structure interaction (SSI) method analyzes a shallow foundation as a rigid body and the surrounding soil as a continuum. It enables modeling of the structure and soil as a single interactive system. Finite-element method (FEM) is a technique based on SSI which allows accurate and detailed evaluation of the soil-foundation system. The first step towards the SSI approach is to determine the static stiffness of the foundation. Our research aims to utilize FEM tools to compute the vertical static stiffness of a rigid tubular foundation and conduct parametric study based on the embedment depth, wall thickness of foundation, and Poisson's ratio of soil. Foundation designs can be optimized and improved in terms of safety and stability by using modern techniques of FEM to determine foundation stiffness using footing parameters like the embedment depth, wall thickness and soil parameters like Poisson's ratio. Gazetas et al. (1985) formulated empirical solutions of static stiffness of rigid foundation by incorporating trench and side wall factors. Aubeny (2023) provides a wall thickness dependent factor for evaluating the static stiffness of a rigid circular footing. Our objective is to compare the existing literature solutions using the principle of superposition with numerically computed values and propose modified equations of vertical static stiffness as a function of the foundation and soil parameters.

ACKNOWLEDGEMENTS

I would like to express my heartfelt gratitude to all those who have supported me in accomplishing my master's research work. I am blessed to have this opportunity and I am grateful to almighty God for the immense mercy and faith.

I would like to start by thanking my advisor Prof. Charles Aubeny, for his guidance, support, and encouragement throughout my journey. His unwavering trust in my abilities and invaluable advice was instrumental in the completion of this thesis. I sincerely appreciate my committee members, Prof. Marcelo Sanchez and Prof. Moo-Hyun Kim, for their supervision and willingness to be a part of my committee.

I would also like to extend my wholehearted regards to my parents, Mrs. Seema B. Grover and Mr. Vikram Jeet Grover, who provided me with love and assurance during the toughest times. Their motivation and understanding have been a source of inspiration to me.

I would like to express my gratitude to Zachry Department of Civil & Environmental Engineering, for providing me with the resources and support I needed to complete this thesis. I would like to acknowledge the National Offshore Wind Research and Development Consortium (NOWRDC), for providing financial support for my research studies.

A very special mention to my dearest friend, Hardik Gupta, who was a constant source of strength and positive influence throughout my graduate degree journey. I am deeply indebted to all the individuals who helped me in my research and provided valuable insights and feedback. This thesis would not have been possible without the help and support of all these individuals, and I am profoundly grateful to each of them.

CONTRIBUTORS AND FUNDING SOURCES

Contributors

This work was supervised by a thesis committee consisting of Prof. Charles Aubeny and Prof. Marcelo Sanchez of the Zachry Department of Civil and Environmental Engineering, and Prof. Moo-Hyun Kim of the Department of Ocean Engineering at Texas A&M University. All work conducted for the thesis was completed by the student independently.

Funding Sources

The graduate studies were partially supported by fellowship from Texas A&M University and graduate assistantship in research role under Prof. Charles Aubeny. This work was made possible by a project ‘Vibratory-Installed Bucket Foundation for Offshore Wind Turbines’ funded by the National Offshore Wind Research and Development Consortium (NOWRDC). The contents of this thesis are solely the responsibility of the author and do not necessarily represent the official views of the sponsors.

NOMENCLATURE

K^* = Vertical dynamic stiffness

$K_{s,e}$ = Vertical static stiffness as a function of embedment depth

$K_{s,t}$ = Vertical static stiffness as a function of wall thickness

a_0 = Frequency parameter

χ_1, χ_2 = Frequency-dependent dynamic multipliers

[B] = Strain matrix

[C] = Stress-strain matrix

[K] = Stiffness matrix

D = Diameter of foundation

E = Young's Modulus of Elasticity

F = Equivalent nodal force

G = Shear Modulus of Elasticity

h = Embedment depth of foundation

I_{tre} = Trench Embedment factor for Foundation Stiffness

I_{wall} = Side Wall Embedment Factor for Foundation Stiffness

K_{emb} = Vertical static stiffness of an embedded foundation

K_s = vertical static stiffness of foundation

K_{s0} or K_{sur} = Vertical static stiffness of foundation at zero embedment i.e at surface

K_{tre} = Vertical static stiffness of the foundation embedded without side wall contact

R = Radius of foundation

R_{in} = Inner radius of tubular foundation

s_f = Wall thickness-dependent shape factor

t = Wall thickness of foundation

U = Nodal displacement

V = Volume of finite element

v_s = Soil shear wave velocity

μ = Poisson's ratio of soil

Ω = Excitation angular frequency

ε = Strain

σ = Total Stress

TABLE OF CONTENTS

	Page
ABSTRACT.....	ii
ACKNOWLEDGEMENTS.....	iii
CONTRIBUTORS AND FUNDING SOURCES	iv
NOMENCLATURE	v
TABLE OF CONTENTS.....	vii
LIST OF FIGURES	ix
LIST OF TABLES.....	xii
1. INTRODUCTION.....	1
1.1 Overview	1
1.2 Offshore Wind Energy	2
1.3 Types of Offshore Foundations.....	2
1.4 Bucket Foundations.....	4
1.5 Vibratory Installation of Bucket Foundations.....	7
1.6 Problem Statement	9
1.7 Outline of Thesis	10
2. THEORY & BACKGROUND.....	12
2.1 Soil-Foundation Interaction.....	12
2.1.1 Soil Behavior	13
2.1.2 Linear Elasticity Constitutive Model.....	14
2.2 Foundation Embedment	15
2.2.1 Trench Effect	18
2.2.2 Sidewall Contact Effect	18
2.3 Continuum Finite Element Concept.....	19
2.3.1 Axisymmetric Stress-Strain Analysis	20

2.3.2	Finite Element Formulation	21
3.	FINITE-ELEMENT MODEL	22
3.1	Model Geometry	22
3.2	Mesh Analysis	24
3.2.1	Elements.....	24
3.2.2	Rigid Body	25
3.2.3	Boundary Conditions	27
3.3	Static Stress Analysis	28
4.	RESULTS.....	31
4.1	Parametric Study	31
4.1.1	Effect of Embedment Depth	33
4.1.2	Effect of Wall Thickness	34
4.1.3	Effect of Poisson’s Ratio	35
4.2	Stress and Displacement Contour Plots	37
4.2.1	Von Mises Stress Contours.....	37
4.2.2	Vertical Displacement Contours.....	40
5.	CONCLUSIONS	44
	REFERENCES	46

LIST OF FIGURES

	Page
Figure 1.1 Cost comparison of onshore and offshore wind power. Reprinted from (Guo et al. 2022).....	1
Figure 1.2 Types of offshore wind turbines foundations with water depth range. Reprinted from (O'Kelly et al. 2016).....	3
Figure 1.3 Monopile of 7.8 diameter used in Veja Mate offshore wind facility. Reprinted from (Skopljak 2016).....	4
Figure 1.4 Embedded tubular foundation. Reprinted from (Abedzadeh and Pak 1995)	5
Figure 1.5 Adjustment of foundation stiffness for embedment effects. Adapted from (Gazetas et al. 1985)	6
Figure 1.6 Typical ranges of embedment factors. Adapted from (Gazetas et al, 1985)	7
Figure 1.7 Framework of vibratory installation of bucket foundation. Reprinted from (Aubeny 2021)	8
Figure 1.8 Vibratory hammer configuration for project OktaKong. Reprinted from (Van Dorp et al. 2019)	8
Figure 1.9 Soil-structure interacting system. Reprinted from (Aubeny 2023)	9
Figure 2.1 Axisymmetric indentation of an isotropic elastic half-space by a rigid circular body. Reprinted from (Boussinesq 1885).....	13
Figure 2.2 Single degree of freedom (SDOF) system. Reprinted from (Lepert et al. 1991)	14
Figure 2.3 Hooke's law for linear-elastic model. Reprinted from (Sture 2004).....	15
Figure 2.4 (a) Surface foundation of arbitrary shape (b) Embedded foundation of arbitrary basemat shape. Reprinted from (Gazetas 1991).....	16

Figure 2.5 Impact of embedment on vertical static stiffness of foundation (a) settlement due to surface foundation (b) trench effect (c) combined trench and sidewall effects. Reprinted from (Gazetas et al. 1985)	19
Figure 2.6 Axially symmetric problem. Reprinted from (Girijavallabhan and Reese, 1968)	20
Figure 2.7 Strains and stresses on an axisymmetric element. Reprinted from (Khennane, 2013)	20
Figure 3.1 Variable sized mesh in ABAQUS	23
Figure 3.2 Four-node element in ABAQUS. Reprinted from (Simulia 2013).....	24
Figure 3.3 Infinite elements in ABAQUS. Reprinted from (Simulia 2013).....	25
Figure 3.4 Rigid body nodes. Reprinted from (Simulia 2013)	26
Figure 3.5 Rigid body nodes for two- and three-dimensional mesh. Reprinted from (Simulia 2013).....	26
Figure 3.6 Convention for degrees of freedom. Reprinted from (Simulia 2013)	27
Figure 3.7 Displacement boundary conditions in ABAQUS.....	28
Figure 3.8 Force control method for static stress analysis.....	29
Figure 3.9 Displacement control method for static stress analysis.....	29
Figure 3.10 Methodology flowchart	30
Figure 4.1 A typical monopile foundation for offshore wind turbine. Reprinted from (Leblanc et al. 2010)	32
Figure 4.2 Comparative plot of embedment factor with embedment depth	33
Figure 4.3 Comparative plot of vertical static stiffness with wall thickness.....	34
Figure 4.4 Effect of Poisson's ratio on embedment factor	35
Figure 4.5 Effect of Poisson's ratio on vertical static stiffness.....	36
Figure 4.6 Stress contour plot for zero embedment ($h/R = 0$)	37

Figure 4.7 Stress contour plot for $h/R = 1$	38
Figure 4.8 Stress contour plot for $h/R = 2$	38
Figure 4.9 Stress contour plot for $h/R = 3$	38
Figure 4.10 Stress contour plot for $t/D = 0.05$	39
Figure 4.11 Stress contour plot for $t/D = 0.25$	39
Figure 4.12 Stress contour plot for $t/D = 0.5$	40
Figure 4.13 Vertical displacement contour plot for zero embedment ($h/R = 0$).....	40
Figure 4.14 Vertical displacement contour plot for $h/R = 1$	41
Figure 4.15 Vertical displacement contour plot for $h/R = 2$	41
Figure 4.16 Vertical displacement contour plot for $h/R = 3$	42
Figure 4.17 Vertical displacement contour plot for $t/D = 0.05$	42
Figure 4.18 Vertical displacement contour plot for $t/D = 0.25$	43
Figure 4.19 Vertical displacement contour plot for $t/D = 0.5$	43

LIST OF TABLES

	Page
Table 3.1 Soil Parameters	23
Table 3.2 Foundation Parameters	24
Table 5.1 Proposed vertical static stiffness equation constants	45

1. INTRODUCTION

1.1 Overview

The energy industry has experienced a huge demand to produce renewable energy owing to the sharp rise in pollution contributed by conventional energy resources. Till the year 2030, renewable energy technologies must grow four times faster than present to curb climate changes and achieve sustainable development goals (McKenna et al. 2022). Wind energy is a rapidly growing form of renewable energy. It can either be produced onshore or offshore. Offshore wind is 50% more expensive than onshore wind based on investment per megawatt (MW) (Wu et al. 2019). Figure 1.1 shows the cost comparison of onshore and offshore wind power production systems (Guo et al. 2022). Wu et al. 2019 also reinforces that foundations account for 20-30% of an offshore wind farm's development based on existing inventory values.

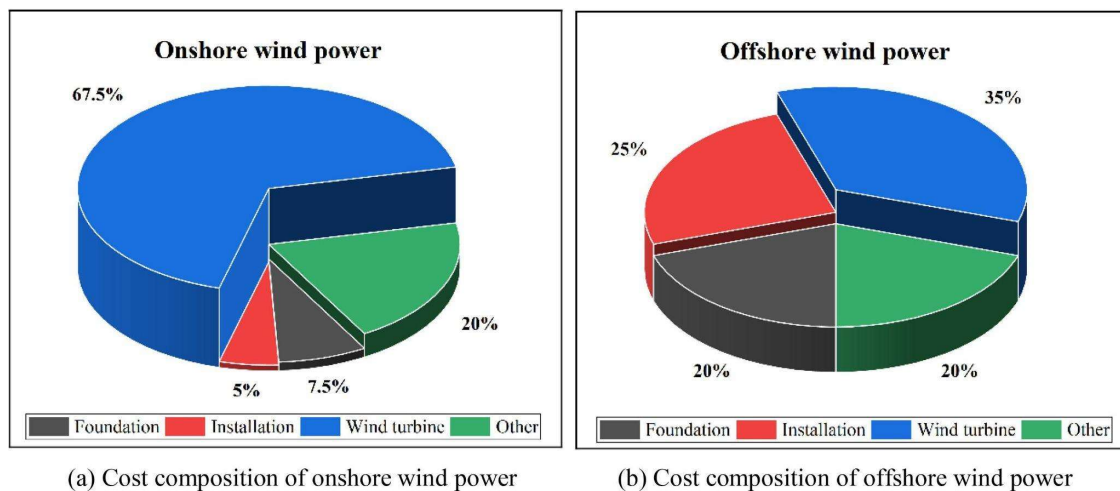


Figure 1.1 Cost comparison of onshore and offshore wind power. Reprinted from (Guo et al. 2022)

The rise in offshore wind turbines (OWTs) indicates the importance of studying and analyzing the foundation design parameters involved. The construction of OWTs, especially their

substructures, is an extremely complex and risky task owing to the mixed composition of loads. This indicates the utmost importance of studying and analyzing OWT's foundation design parameters to avoid failures.

1.2 Offshore Wind Energy

Wind energy production is not only aligned with the climate change concerns but has huge commercial development potential. Most countries have largely developed onshore wind energy owing to the hindrances in transportation, installation, wind turbine technology, and policy orientation techniques in offshore wind energy. However, offshore wind energy has been proved to have certain advantages over onshore wind energy. Offshore wind can be deployed for large capacity wind turbines unlike onshore wind. The service life of offshore wind towers is longer since they are not affected by difficult terrains leading to airflow disruptions, and they experience less fatigue load given the low intensity of turbulence. The rate of energy utilization of offshore wind is higher as compared to onshore wind majorly because of the low surface roughness of development areas. In environmental terms, offshore wind energy farms are located far from human impact ecological zones, resulting in safer energy production. (Guo et al. 2022) The west and east coast of the United States of America is considered significant for offshore wind energy resources in the 21st century especially for climate change decisions (Costoya et al. 2020).

1.3 Types of Offshore Foundations

The type of foundation varies with each project depending upon the location, depth of installation, energy requirements, etc. Sánchez et al. (2019) states the importance of correct typology of offshore foundations to minimize costs and maximize performance. These factors include meter ocean climate, distance to coast, unexpected calamities like tsunami, earthquakes, etc. and depth.

There are several types of foundations available for OWTs like monopile foundations, floating foundations, tripod foundations, gravity foundations, and bucket foundations (Wang et al. 2018).

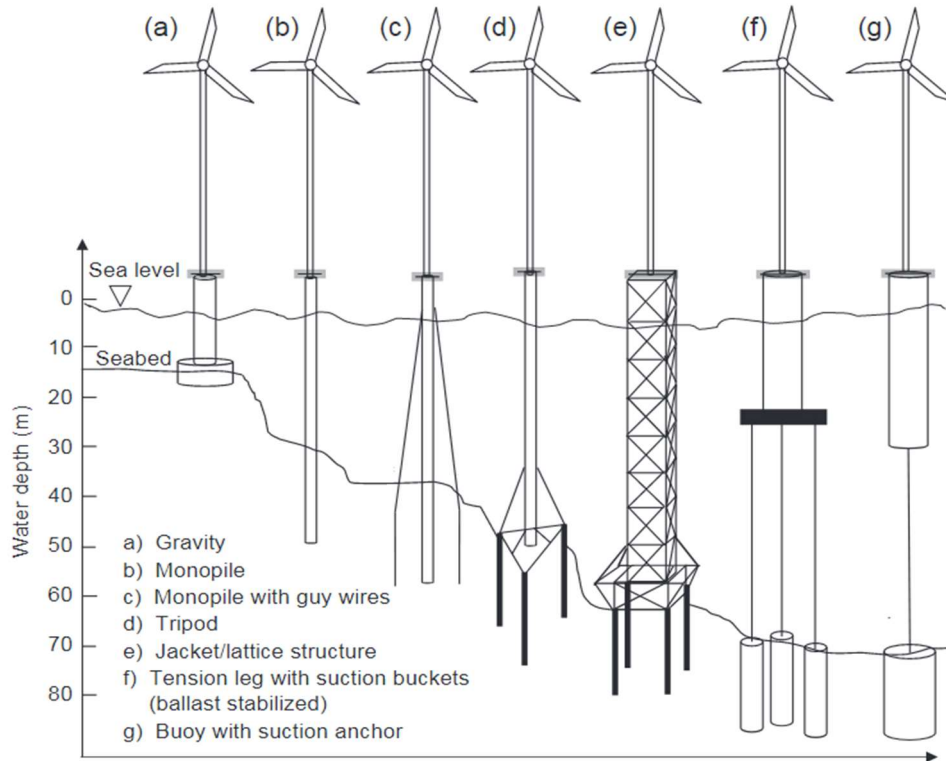


Figure 1.2 Types of offshore wind turbines foundations with water depth range. Reprinted from (O'Kelly et al. 2016)

Monopiles are foundations made up of cylindrical steel tubes. Their popularity in offshore wind farms throughout the world is due to the simplicity in design, construction, installation, and maintenance. Monopiles do not require cutting edge technologies which reduces the cost and time of installation and construction without compromising the durability and safety. They adapt to a large range of depths and do not require intense field data (Sánchez et al. 2019).



Figure 1.3 Monopile of 7.8 diameter used in Veja Mate offshore wind facility. Reprinted from (Skopljak 2016)

1.4 Bucket Foundations

Bucket foundations are shell-like structures that are driven or sunk into the ground to provide high-bearing capacity and stability to offshore structures, especially wind turbines. Bucket foundations offer a lucrative alternative to long pile foundations like monopiles due to their low length-to-diameter ratio, termed as aspect ratio. The cost of transportation and installation of the bucket foundations is lesser as compared to long monopiles. Additionally, there exists a possibility for fabricating a monolithic unit consisting of the wind tower superstructure and the bucket foundation which can further reduce the expenses without compromising on the safety.

This research aims to model a short tube foundation by studying a finite cylindrical structure embedded in a semi-infinite elastic half-space. Numerical solution of an embedded short cylindrical body provides a realistic model for structures used in offshore and naval industries like hollow piers and suction anchors (Abedzadeh and Pak 1995).

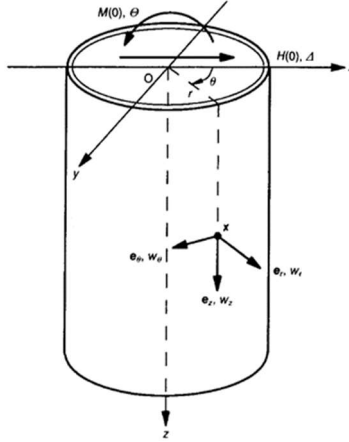


Figure 1.4 Embedded tubular foundation. Reprinted from (Abedzadeh and Pak 1995)

An axisymmetric two-dimensional elastic half-space model is the most efficient and easiest way to physically model a rigid tubular foundation embedded in a linear, elastic, homogeneous and isotropic soil continuum. Elasticity theory, in the context of foundations, states that the deformations are directly proportional to the stresses experienced by footings under loads. Roesett (1980) provided the mathematical relationship for evaluating static stiffness, K_s of a rigid disk resting on a homogeneous elastic half-space by studying the relationship between force and displacement.

$$K_s = \frac{4GR}{1 - \mu}$$

where G is the shear modulus of soil, μ is soil Poisson's ratio, and R is the foundation radius. The derivation of stiffnesses of soil-foundation systems are significant for studying the dynamic soil-structure interaction effects especially in the seismic design of nuclear power plants (Kausel and Roesett 1975). Static stiffness estimations can aid geotechnical engineers in predicting failure of foundations. High values of stiffness indicate efficient transfer of loads; however, it also signifies resistance to lateral loads like wind loads, or earthquakes, etc. Hence, a structure's stability and serviceability can be accurately evaluated using these studies.

In real-life structures, foundations are not placed on the surface. They are installed at a certain depth below the surface of ground which increases the bearing capacity, uplift resistance, stability and decreases the settlement of structures. Gazetas et al. (1985) offers approximate expressions for defining the relationship of increased foundation embedment in half-space resulting in a rise of foundation stiffness. It includes two factors, trench factors I_{tre} and wall factor I_{wall} . Trench factor, I_{tre} characterizes the impact of load application point within the soil mass while wall factor, I_{wall} characterizes the effect of a rigid as opposed to free boundary condition on the side walls of the trench (Figure 1.5). Embedment factors, I_{tre} for trench effect is 0.095 and I_{wall} for wall effect is 0.19, are provided by Gazetas et al. (1985). Figure 1.6 depicts the plot for embedment factors for embedment depth varying from 0 to 3. The formulas for embedment factors are as below.

$$I_{tre} = 1 + \frac{2}{21} \frac{h}{R}$$

$$I_{wall} = 1 + 0.19 \left(\frac{2D}{B} \right)^{2/3}$$

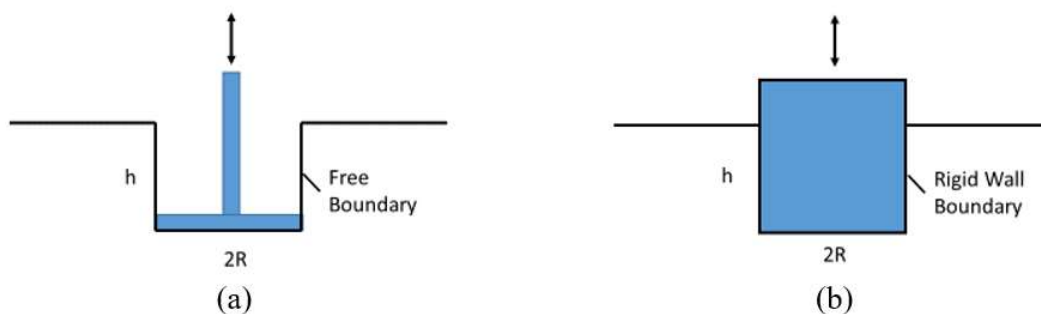


Figure 1.5 Adjustment of foundation stiffness for embedment effects. Adapted from (Gazetas et al. 1985)

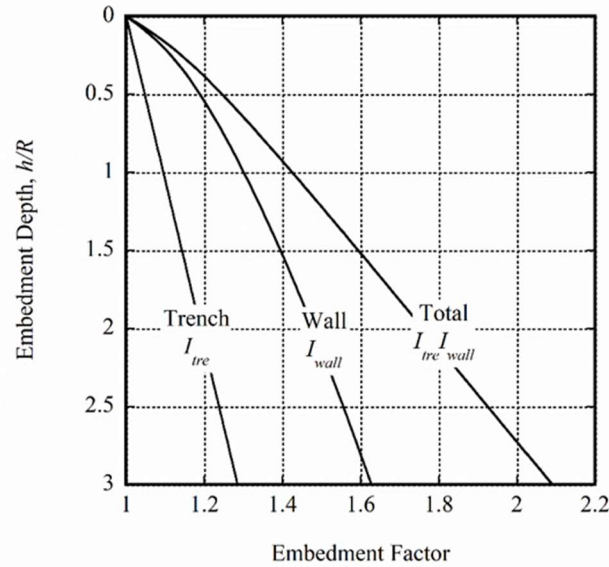


Figure 1.6 Typical ranges of embedment factors. Adapted from (Gazetas et al, 1985)

1.5 Vibratory Installation of Bucket Foundations

There are majorly two methods of installing a bucket foundation: vibratory or suction. Suction-installed bucket foundations have been widely researched and utilized in the arena of offshore wind farms. However, there are certain advantages of vibratory installation which must be considered. These include (1) reduction of installation time in minutes in comparison to hours (2) lesser noise pollution as opposed to impact hammers used for pile driving (3) viability in heterogeneous soil profiles unlike suction installation (4) decreased driving stresses leading to lesser chances of failure; and (5) possibility of extracting and reposition of foundation (Aubeny 2023).

Figure 1.7 is a schematic representation of the OWT bucket foundation installed by vibratory hammers at the platform. Figure 1.8 is an offshore foundation monopile installed using vibratory hammers for windfarm used for project OcktaKong in Macau (Van Dorp et al. 2019).

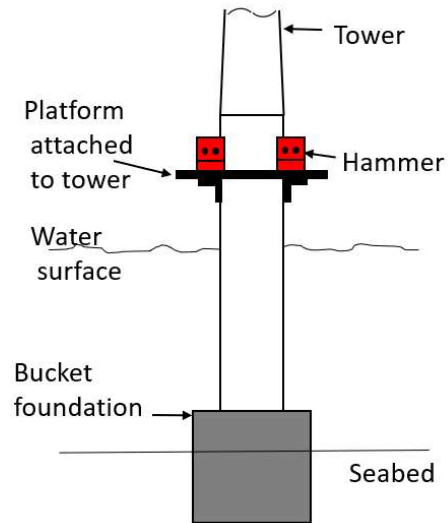


Figure 1.7 Framework of vibratory installation of bucket foundation. Reprinted from (Aubeny 2021)



Figure 1.8 Vibratory hammer configuration for project OktaKong. Reprinted from (Van Dorp et al. 2019)

The following equation determines the dynamic stiffness of a shallow foundation at the surface of an elastic half-space medium.

$$K^* = K_s(\chi_1 + i a_0 \chi_2)$$

Where a_0 is the frequency parameter calculated by the formula

$$a_0 = \frac{\Omega R}{v_s}$$

In this thesis, we focus on estimating the static stiffness of the bucket foundation which can be utilized for determining the dynamic stiffness contributing towards the vibratory installation.

1.6 Problem Statement

The primary goal of this thesis is to develop a finite element model of a rigid tubular foundation embedded in an elastic homogeneous half-space for offshore wind turbines to conduct static vertical stiffness analysis based on soil structure interaction concept. Simplistic models like axisymmetric and two-dimensional are best suited for preliminary analysis and are computationally less demanding. The symmetry about an imaginary axis of the rigid tubular foundation allows for a decrease in the degrees of freedom of the structure giving rise to a more efficient and less time-consuming analysis. The soil-structure interaction of a shallow foundation with an underlying elastic half-space is typically described by a single degree spring-mass-dashpot single-degree-of-freedom (SDOF) system for dynamic analysis as shown in Figure 1.9. The system includes a mass (representing the foundation), a spring (representing the stiffness of soil), and a dashpot (representing the damping of soil). This system is useful in predicting the response of shallow offshore foundations for vibratory hammers utilized for installation.

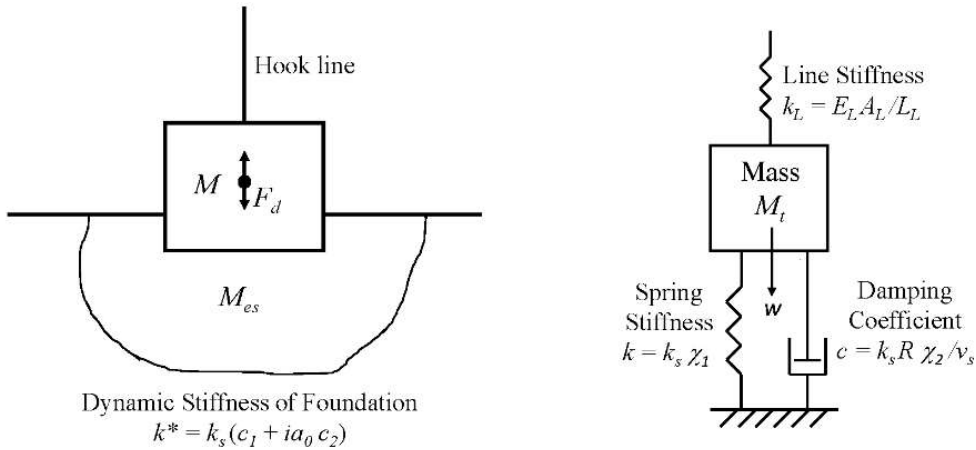


Figure 1.9 Soil-structure interacting system. Reprinted from (Aubeny 2023)

The FEM software package ABAQUS 6.24 (Simulia 2013) has been deployed to perform the vertical static stiffness analysis of the embedded tubular foundation. The main objectives of the thesis are as follows:

1. To generate an axisymmetric two-dimensional linear elastic FEM model of a rigid tubular foundation embedded in a homogeneous isotropic elastic half-space.
2. To determine the impact of the depth of embedment, wall thickness of foundation, and Poisson's ratio of surrounding soil on the vertical static stiffness of foundation.
3. To perform comparative studies between existing solutions in the literature with our FEM based integrated values of static stiffness.
4. To propose modified equations incorporating the effect of embedment depth, wall thickness, and Poisson's ratio on vertical static stiffness of footing.

1.7 Outline of Thesis

The thesis has been classified into five comprehensive chapters. The contents have been explained briefly as follows.

Chapter 2: Theory & Background

This chapter revolves around the fundamental literature review conducted for our research work. It begins with understanding the concepts of soil-foundation interaction. It focuses on the advantages of linear elastic constitutive soil model and the impact of soil behavior on the mechanical response. The next section discusses the real-life process of installation of foundations beneath a certain depth referred to as embedment depth. There are two adjustment factors, trench factor and side wall factor, developed for calculating the foundation stiffness at specific embedment depth. The third section revolves around the topic of continuum soil mechanics and

discretization of finite elements. It describes the use of axisymmetric models for simplifying complex stress-strain analysis of large structures.

Chapter 3: Finite Element Model

This chapter is a guide to the methodology adopted for our static stiffness studies. It begins with describing the geometry of our two-dimensional axisymmetric model. The next session discusses development of a suitable mesh on ABAQUS 6.24 (Simulia 2013) software package. It covers the types of elements and boundary conditions utilized for our FEM model and the concept of using a rigid body function. The last section emphasizes on force and displacement control methods to determine the static stiffness of the rigid foundation.

Chapter 4: Results

This chapter provides the results for the parametric study conducted based on embedment depth, wall thickness of foundation, and Poisson's ratio of soil. It contains graphs which give an insight into

the variation of vertical static stiffness of foundation determined through Gazetas et al. 1985 solutions and our FEM model. The next section is dedicated to the displacement and stress contours for various cases modelled for our analysis.

Chapter 5: Conclusions

This chapter concludes by stating some key observations and inferences from our numerical studies for a rigid tubular foundation. It proposes a modified equation based on the parametric study which incorporates the impact of embedment depth, foundation's wall thickness, and Poisson's ratio of soil.

2. THEORY & BACKGROUND

2.1 Soil-Foundation Interaction

Major engineering applications involve studying the interaction between two deformable bodies. A large portion of these interaction problems are fundamentally related to elastic interaction which are extended to material properties like inelastic, nonlinear elastic, and time-dependent behaviors. The interaction of elastic bodies is analyzed by individually investigating the stresses and strains experienced along with the distribution of stresses and displacements at the contact areas. There are three cases which can be utilized to analyze the interaction of deformable elastic media: interaction between elastic bodies; interaction between an elastic medium and rigid body, and interaction between elastic bodies and structural elements. The realm of soil mechanics and foundation engineering is extensively concerned with the third category dealing with interaction between structural elements like beams, foundations on linearized deformable elastic media. (Selvadurai 2013)

Boussinesq published a book in 1885 which, for the very first time, provided a solution to evaluating the state of stress in a homogeneous, isotropic, elastic half-space because of deformation caused by a rigid smooth object. Figure 2.1 presents the axisymmetric problem in which the axis of deforming rigid circular solid is orthogonal to the undisturbed boundary of elastic half-space.

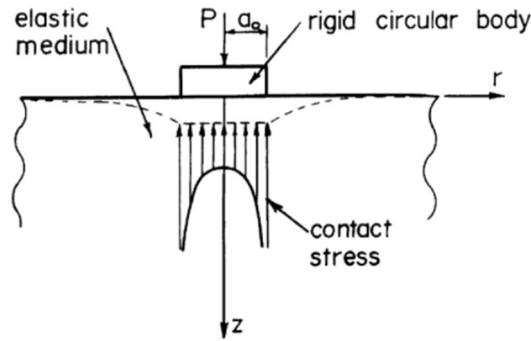


Figure 2.1 Axisymmetric indentation of an isotropic elastic half-space by a rigid circular body. Reprinted from (Boussinesq 1885)

Soil-structure interaction studies basically focus on interdependence of the response of soil to load imposed by the foundation and the response of the foundation to the resulting deformations in the soil media. It has a vast number of applications in geotechnical engineering like seismic analysis, flexible pavement design, offshore foundation design, and so on. The stiffness of foundation plays a crucial role in solving any soil-foundation interaction study. High foundation stiffness indicates efficient transfer of loads with less deformations and settlements. However, stiffer foundations can result in stress concentrations posing a risk of failure. This research contributes towards stiffness analysis based on FEM; a methodology based on soil-structure interaction concept.

2.1.1 Soil Behavior

There are several factors which influence the mechanical response of naturally occurring soils including the size and shape of soil particles, soil arrangement, pre-consolidation stresses, permeability, and so on. The stress-strain relationship varies with these factors leading to soil nonlinearity, anisotropy, non-homogeneity, and time-dependent properties. It is a complex task to account for such soil material properties to achieve soil-foundation interaction modeling. Idealization of soil behavior contributes towards a reliable and practical solution to the complicated soil-foundation problem. The most straightforward method is to assume a linear-elastic behavior

of the surrounding soil media. It certainly does not represent the natural characteristics of soils in real-life. However, past research indicates that linearized elastic behavior of soil provides reasonable estimations of the soil response at minimal computational efforts (Selvadurai 2013). Lepert et al. (1991) considers the “soil + foundation” system as a single degree of freedom (SDOF) mechanism as shown in Figure to estimate the soil stiffness under a rigid spread foundation assuming an elastic soil model. It yields that the in-situ laboratory results match their empirical results.

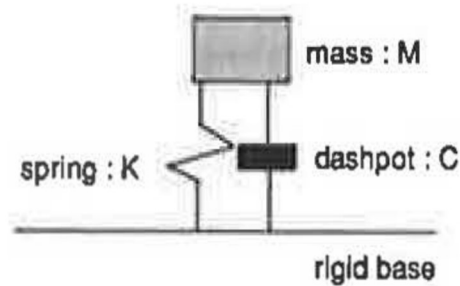


Figure 2.2 Single degree of freedom (SDOF) system. Reprinted from (Lepert et al. 1991)

2.1.2 Linear Elasticity Constitutive Model

A linear elastic soil model means that strains or response to stresses are proportional to applied stresses and the material returns to its original state upon removal of stresses. Elasticity in soil is the most basic model which assumes isotropy and homogeneity along with linearity and elasticity. Isotropy in soil indicates that the properties of soil are the same in all directions. Irrespective of the orientation of soil particles, it has constant mechanical properties, like stiffness, throughout the media. Spatial uniformity is featured in homogeneous soils meaning that it consists of the same material throughout. It is an assumption used typically by FEM systems to simplify analyses and achieve practical estimations of soil characteristics like load bearing capacity, stiffness, and so on.

Two parameters, Young's Modulus and Poisson's ratio are fundamental characteristics for soil elasticity models. Figure 2.3 indicates the proportionality between stress and strain for linear elastic soil models with no hysteresis which is called Hooke's Law. The slope of the plot is a constant of proportionality referred to as the soil's Young's Modulus of Elasticity.

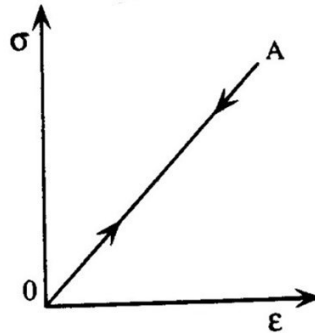


Figure 2.3 Hooke's law for linear-elastic model. Reprinted from (Sture 2004)

The following exhibits Hooke's law for linear isotropic elastic materials where there are only two parameters of interest, i.e Young's Modulus and Poisson's ratio. (Brinkgreve 2005)

$$\begin{bmatrix} \sigma_{xx} \\ \sigma_{yy} \\ \sigma_{zz} \\ \sigma_{xy} \\ \sigma_{yz} \\ \sigma_{zx} \end{bmatrix} = \frac{E}{(1 - 2\mu)(1 + \mu)} \begin{bmatrix} 1 - \mu & \mu & \mu & 0 & 0 & 0 \\ \mu & 1 - \mu & \mu & 0 & 0 & 0 \\ \mu & \mu & 1 - \mu & 0 & 0 & 0 \\ 0 & 0 & 0 & \frac{1}{2} - \mu & 0 & 0 \\ 0 & 0 & 0 & 0 & \frac{1}{2} - \mu & 0 \\ 0 & 0 & 0 & 0 & 0 & \frac{1}{2} - \mu \end{bmatrix}$$

Shear modulus of elasticity, G , of such a soil model is defined by the relationship below.

$$G = \frac{E}{2(1 + \mu)}$$

2.2 Foundation Embedment

Foundations are installed or buried to a certain depth below the surface of ground to transfer the loads to soil beneath. The embedment depth is determined by a multitude of factors like soil type,

loading conditions, standard codes, and so on. The response of embedded foundations subjected to loads is of great practical importance to geotechnical studies especially for OWTs. Numerous studies have concluded that embedment considerably increases the static stiffness of foundations (Gazetas et al. 1985 ; Kausel and Roesset 1975 ; Kausel and Ushijima, 1977). Figure 2.4 (a) presents a schematic diagram of an arbitrary shaped rigid massless surface foundation. Figure 2.4 (b) depicts the same foundation embedded in homogeneous half-space medium. (Gazetas 1991)

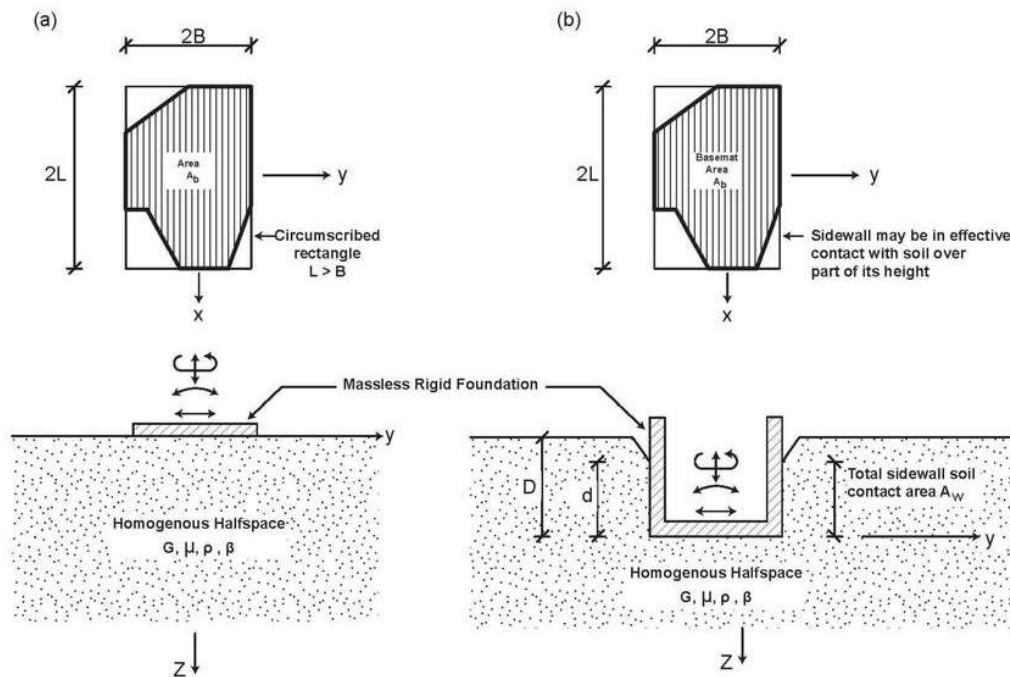


Figure 2.4 (a) Surface foundation of arbitrary shape (b) Embedded foundation of arbitrary basemat shape. Reprinted from (Gazetas 1991)

Surface foundations characterize zero embedment case which is studied for calculating the static stiffness of the foundation with no embedment. This serves as a normalizing factor for vertical stiffnesses at various embedment depths. Embedment factor is the ratio between static stiffness at an embedment depth ratio, h/R and static stiffness of surface foundation or zero embedment (at $h = 0$).

$$\text{Embedment Factor} = \frac{K_s}{K_{s0}}$$

For a circular footing with zero embedment, the static stiffness for vertical loading can be expressed by the following equation (Aubeny 2023).

$$K_{s0} = \frac{s_f GR}{(1 - \mu)}$$

where s_f is the wall thickness-dependent shape factor and is determined by the formula below.

$$s_f = 2.6464 t/D + 13.024 (t/D)^{0.5} - 0.6157$$

The shape factor is equal to 4 for a solid rigid circular foundation (Roesset, 1980). It is theoretically possible to calculate a shape factor for a tubular foundation with outer radius R and inner radius R_i , with the latter being subtracted from the former, by superimposing the solutions for rigid disks. This answer, however, would indicate that there would be no ground displacement interior of the foundation. The superposition of solutions for evenly weighted areas of outer radius R and inner radius R_i yields a more realistic solution. The author derives the shape factor equation s_f empirically for an annular loaded area based on the superposition of Poulos and Davis (1974) solutions for circular regions with homogeneous stress intensity. The shape factor lies anywhere from 3.75 at $D/t = 2$ (a solid area) to 0.3135 for $D/t = 200$. The former value associates to 4 for a solid circular rigid footing (Roesset, 1980).

There are no direct empirical solutions available for determining the vertical static stiffness of embedded tubular foundations. The principle of superposition is utilized to calculate the static stiffness of the tube-structure at the surface. Through our research, we aim to analyze, compare, and propose the effect of embedment depth, wall thickness, and Poisson's ratio on the static stiffness of a rigid massless tubular foundation.

2.2.1 Trench Effect

The trench effect is a result of reduced settlement caused by increased normal and shearing stresses by the enveloping soil. The rise of vertical static stiffness restricts movement of the structure axially. K_{tre} refers to the vertical static stiffness of the foundation embedded without side wall contact. The ratio of K_{tre} and K_{sur} is termed as the trench factor which is always greater than 1. (Gazetas et al. 1985)

$$\frac{K_{tre}}{K_{sur}} = I_{tre} > 1$$

2.2.2 Sidewall Contact Effect

The sidewall effect is a result of the contact between vertical sidewall and soil through which applied load is transferred resulting in shear stresses along the sides. The static stiffness of such an embedded foundation, K_{emb} , is more than an embedded foundation with trench and no sidewalls, K_{tre} . The following provides the dimensionless sidewall-contact factor, I_{wall} as the ratio of K_{emb} and K_{tre} . (Gazetas et al. 1985)

$$\frac{K_{emb}}{K_{tre}} = I_{wall} > 1$$

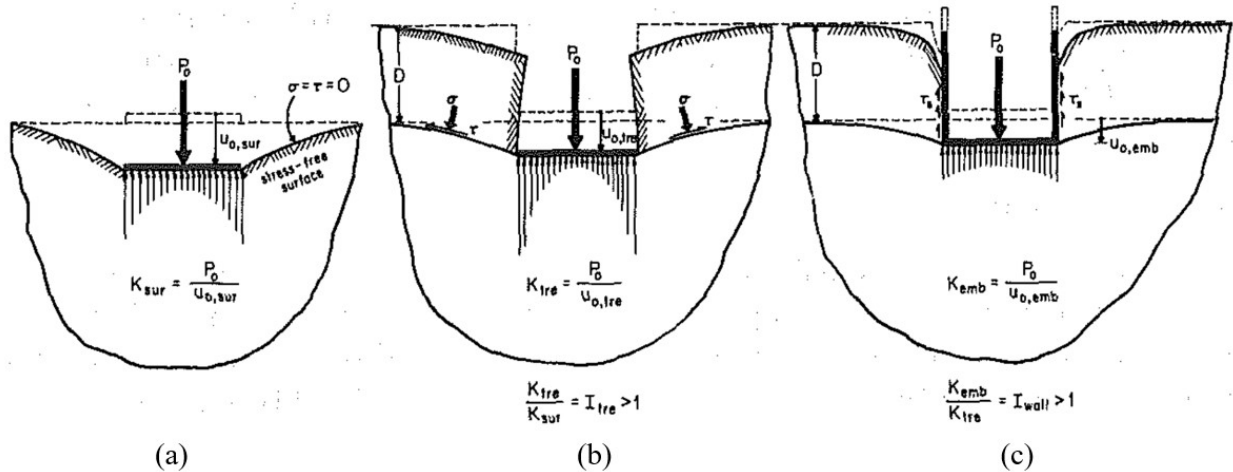


Figure 2.5 Impact of embedment on vertical static stiffness of foundation (a) settlement due to surface foundation (b) trench effect (c) combined trench and sidewall effects. Reprinted from (Gazetas et al. 1985)

The above equations can be combined for calculating the vertical static stiffness of an embedded foundation if the vertical static stiffness of the surface foundation is known by using the following relationship.

$$K_{emb} = K_{sur} \cdot I_{tre} \cdot I_{wall}$$

2.3 Continuum Finite Element Concept

Continuum soil mechanics is based on the concept that soil is a continuous media. It is relevant to homogeneous and isotropic material since it considers continuously varying properties. This assumption enables discretization of the continuum into finite elements. These elements are interconnected by key points referred to as nodes. Each element can then be analyzed for the soil behavior by utilizing constitutive modeling. The continuum finite element formulation studies the interaction between soil elements through equations based on the behavior of soil in response to imposed stresses. It is useful in predicting the performance of structures subjected to various load combinations, both statically and dynamically.

2.3.1 Axisymmetric Stress-Strain Analysis

Axisymmetric linear elastic model based on linear elastic parameters, Young's modulus and Poisson's ratio, has been developed for our research towards embedment of a tubular foundation. Three-dimensional problems can be easily solved through an axisymmetric system with the ease of computational efforts and time of a two-dimensional model. Figure 2.6 is a representation of axial symmetry for a continuum media with assemblage of discrete elements.

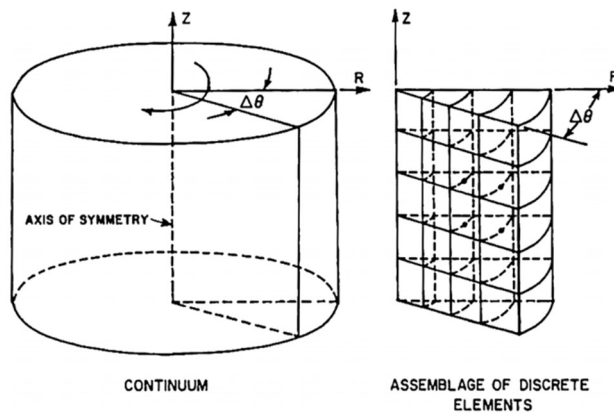


Figure 2.6 Axially symmetric problem. Reprinted from (Girijavallabhan and Reese, 1968)

Figure 2.7 depicts the orientation and representation of stresses and strains acting on any element of an assumed axisymmetric structure.

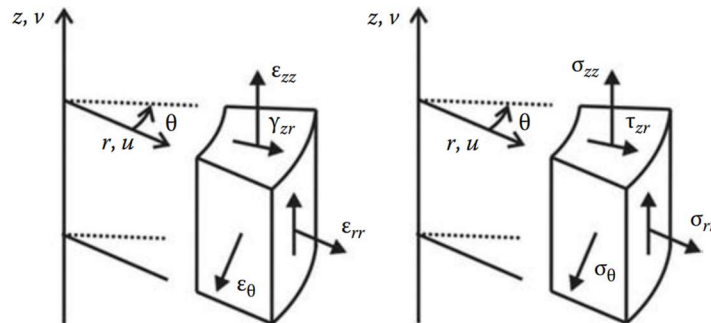


Figure 2.7 Strains and stresses on an axisymmetric element. Reprinted from (Khennane, 2013)

2.3.2 Finite Element Formulation

Bathe 1982 proposed the stress strain matrix, [C], by giving the following relationship between stress and strain.

$$\{\sigma\} = [C] \{\varepsilon\}$$

The stiffness matrix [K] of an element is determined by multiplying the stress-strain matrix [C] with the strain matrix [B] and the transpose of strain matrix [B]^T, and then integrating over the volume of the element, V.

$$[K] = \int_V [B]^T [C][B] dV$$

The resultant derived from the finite element equations are solved to obtain the following relationship.

$$[K]\{U\} = [F]$$

Where $\{\delta\}$ is nodal deformation vector and [R] is the vector of equivalent nodal forces for the element. For a single node, this relationship can be simplified to calculate the static stiffness.

$$K_s = \frac{F_y}{U_y}$$

Where F_y is the equivalent nodal force in the y-direction and U_y is the displacement in y-direction.

3. FINITE-ELEMENT MODEL

Our study is based on an asymmetrical two-dimensional model of a massless rigid tubular footing embedded in a homogeneous and isotropic elastic half-space. Simplistic models like axisymmetric and two-dimensional are best suited for preliminary analysis and are computationally less demanding. The symmetry about an imaginary axis of the rigid tubular foundation allows for a decrease in the degrees of freedom of the structure giving rise to a more efficient and quicker analysis. This chapter is an overview of finite element analysis (FEA) of the embedded rigid tubular foundation conducted in ABAQUS (Simulia 2013), a commercial software. The FEA software provides solutions for a variety of engineering problems by simulating mechanical, thermal, and coupled multi-physics problems. It supports standard and explicit FEA with integrated tools for pre- and post-processing requirements for model generation, analysis setup, and output visualization.

3.1 Model Geometry

This research utilizes a rigid axisymmetric tube foundation in a linear elastic, isotropic, homogeneous soil with a constant Young's Modulus and Poisson's ratio. Since the loading conditions are purely vertical with no lateral loads involved, a two-dimensional axisymmetric model is deployed. For any FEM model, the first step involves creating a discretized representation, referred to as mesh, of the structure's geometry based on the problem statement. There is a significant impact of mesh quality on the accuracy of the results. Finer mesh i.e high nodal density is deployed at regions of embedment since it enables precise material behavior analysis. The elements towards the boundaries may have a coarser mesh since it has a less critical material behavior, and it aids in faster and feasible computation. This study utilizes MATLAB programming tools to define a variable sized mesh as shown in Figure 3.1.

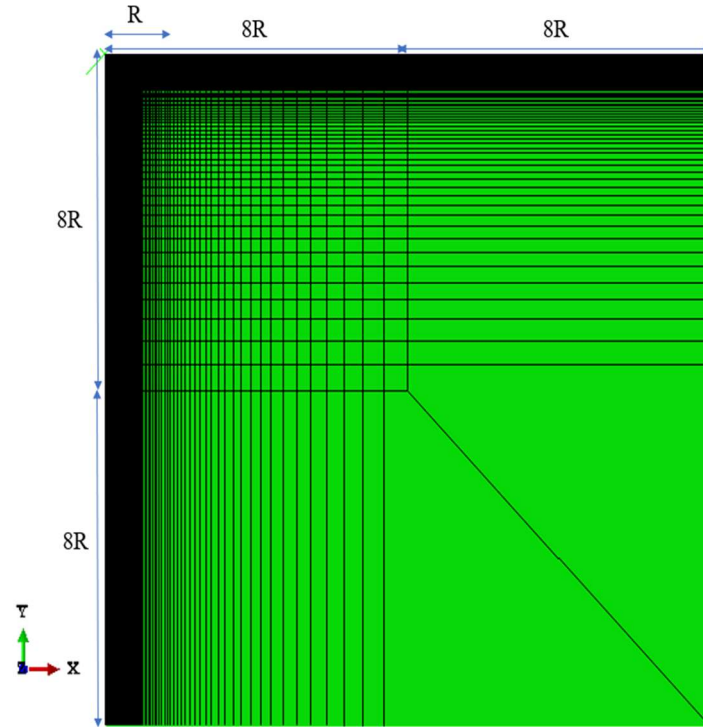


Figure 3.1 Variable sized mesh in ABAQUS

Table 3.1 provides the material properties of the soil used for our parametric study on depth of embedment and wall thickness. For studying the effect of Poisson’s ratio, the range of Poisson’s ratio is 0.25 to 0.45. These values have been used based on the literature review of our research work. The Young’s modulus of foundation is selected high as compared to soil, since we are assuming a rigid foundation.

Table 3.1 Soil Parameters

Soil Parameters	Value
Young’s Modulus of Soil (Pa)	1000
Poisson’s Ratio	0.35
Shear Modulus of Elasticity (Pa)	370

Table 3.2 gives a record of the foundation parameters utilized for developing our two-dimensional axisymmetric model in ABAQUS.

Table 3.2 Foundation Parameters

Foundation Parameters	Value
Diameter (m)	2
Poisson’s Ratio	0.35
Young’s Modulus of Soil (GPa)	200

3.2 Mesh Analysis

3.2.1 Elements

The element library available in ABAQUS/Standard has a diversity of element types that aid in meshing of the soil domain. CAX4 is a four-node bilinear section element which experiences stresses and displacements without twist. These elements are two-dimensional, solid continuum (C) axisymmetric (AX) stress and displacement components with full integration along with first-order interpolation as shown in Figure 3.2.

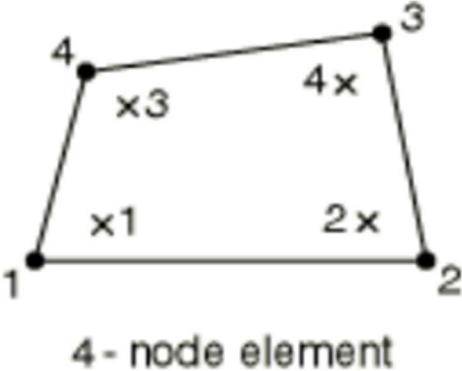


Figure 3.2 Four-node element in ABAQUS. Reprinted from (Simulia 2013)

Each node in a CAX4 element has two active degrees of freedom ie. displacement in the x-direction and displacement in the y-direction. Any CAX4 element can be established by specifying coordinates of the nodal points in counterclockwise direction as shown in Figure 3.2.

Infinite elements are components used in unbounded domains where the area of interest is small in comparison to the surrounding medium. They are used in combination with finite elements as depicted in Figure 3.3.

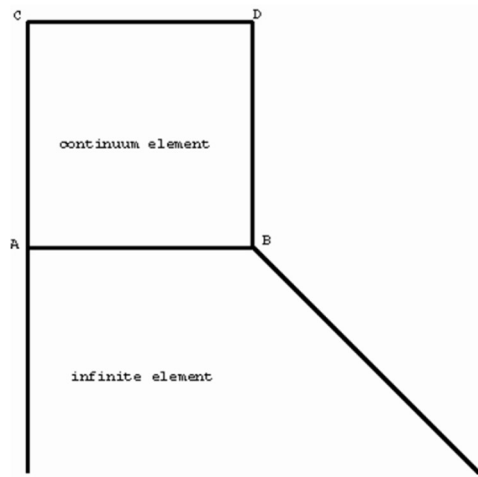


Figure 3.3 Infinite elements in ABAQUS. Reprinted from (Simulia 2013)

3.2.2 Rigid Body

Rigid bodies can simply be defined as ideal objects that do not change shape or have zero deformation. In an FEM model, they are basically a group of nodes, elements, and/or surfaces which act together. The movement of these nodes, elements, and/or surfaces is ruled by a single node, referred to as the reference node of the rigid body. Throughout the analysis, there is no change in the relative displacement of the nodes and elements which constitute the rigid body.

Figure 3.4 is a representation of elements that compose a rigid body. The rigid slave nodes denote that they are governed by the rigid body reference node.

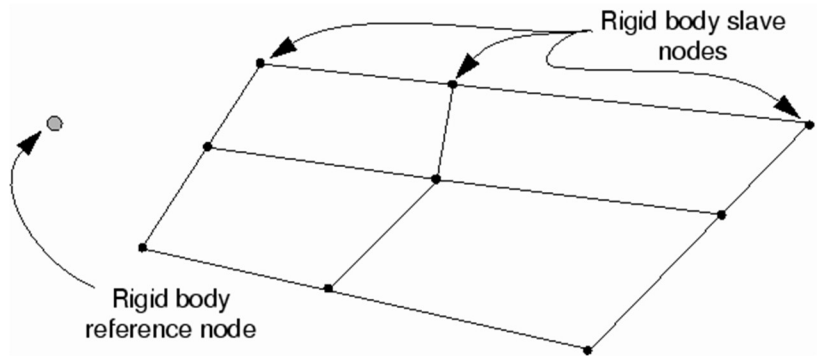


Figure 3.4 Rigid body nodes. Reprinted from (Simulia 2013)

Rigid body tool in ABAQUS software is specifically effective for studying stiff regions in a model that can majorly contribute towards computational competence. It commands the processor to avoid focusing on tracking the waves and stress distributions of the components defined as a rigid body. Figure 3.5 depicts three-dimensional rigid bodies utilized to restrict two finite element solids at the interface.

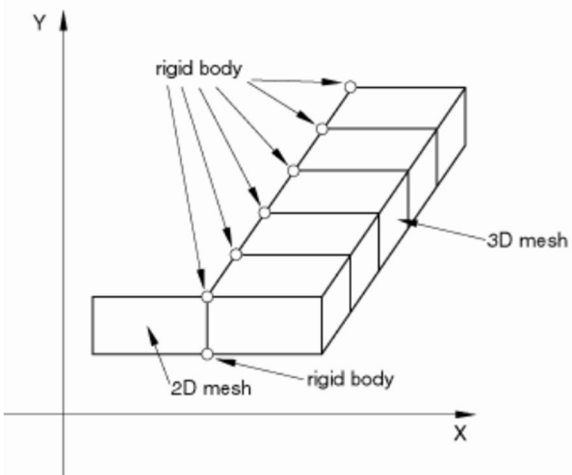


Figure 3.5 Rigid body nodes for two- and three-dimensional mesh. Reprinted from (Simulia 2013)

Boundary conditions, as explained in the next subsection, are deployed at the rigid body reference node to characterize movement of the rigid body. Concentrated loads applied to nodes and distributed loads applied to elements of the rigid body generate stresses and displacements. The interaction of rigid bodies with the rest of the model is crucial for analyzing behavior of the structure. The empirical solutions our model compares are based on rigid circular foundation, hence, we use rigid body function for defining the tubular foundation.

3.2.3 Boundary Conditions

Boundary conditions are utilized to describe values at nodes of fundamental variables like displacement, pore pressure, temperature, electrical potential, etc. They can also be deployed as model input or history input data to set boundary conditions of zero value or edit non-zero and zero-value boundary conditions. (Simulia 2013). Our model utilized displacement boundary conditions to restrict lateral movement along the axis of symmetry. The directions in which a node is free to move is referred to as degrees of freedom (dof). The convention used In ABAQUS for degrees of freedom are shown in Figure 3.6. In our model, the boundary conditions direct zero rotational displacements since our focus is on translational motions only.

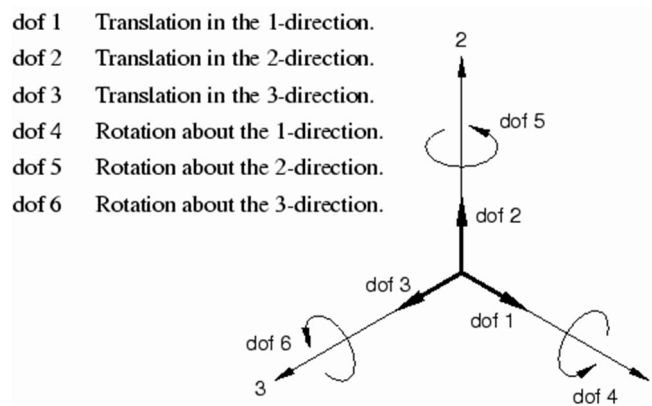


Figure 3.6 Convention for degrees of freedom. Reprinted from (Simulia 2013)

Figure 3.7 is a representation of the restricted x-direction displacement for the centerline of the foundation along with constrained rotational displacement of the rigid body reference node (blue arrows). No boundary conditions are set at the bottommost and outermost part of the model since infinite elements have been stationed at the far-field regions.

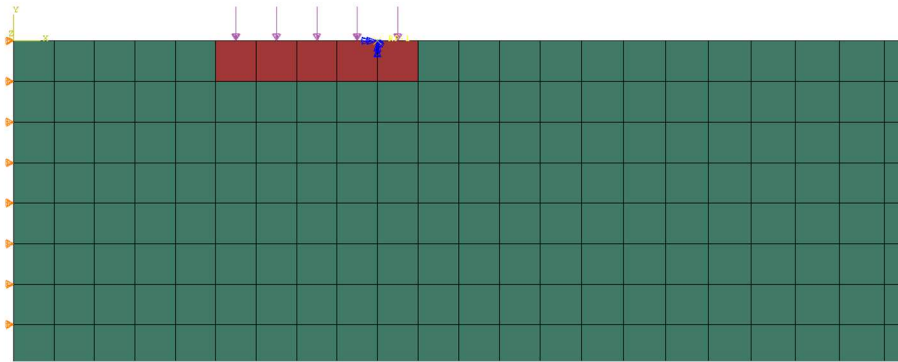


Figure 3.7 Displacement boundary conditions in ABAQUS

3.3 Static Stress Analysis

Large computational costs and time can be reduced by utilizing the linear static stress analysis step for evaluating static stiffnesses. It is an effective simulation technique where inertia effects and time-dependent material effects can be neglected for the model. Our model is designed to study the effect of embedment and wall thickness on the tubular foundation. A linear static step is defined in the FEM software to characterize the loads and boundary conditions on elements and nodes forming the foundation.

The static step is suited for mechanical behavior models of materials like elasticity soil models. A suitable time period is required for the static analysis because it aids cross-referencing of amplitude parameters, especially varying loads. By default, it is considered a single unit for constant loading cases. Element outputs of stress, strain, energy and nodal outputs of displacement, reaction forces, coordinates can be generated. There are two approaches that can be followed for the static stress

analysis: force control and displacement control. In force control, a known magnitude of force or pressure is applied to generate deformation. This is useful for studying the linear response of soil. On the other hand, displacement control method involves applying a known displacement and measuring the output of force or stress. Figure 3.8 shows a static analysis case utilizing force control method for an assumed surface tubular foundation. Figure 3.9 shows displacement control method by embedding nodes of interest to characterize an embedded tubular foundation.

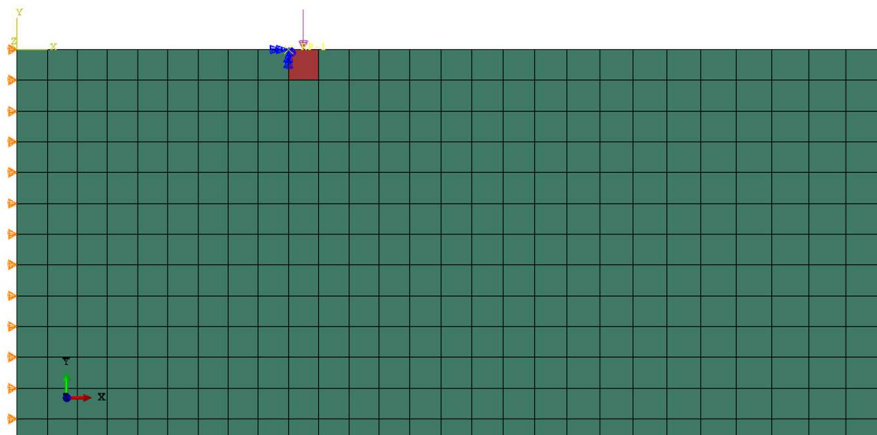


Figure 3.8 Force control method for static stress analysis

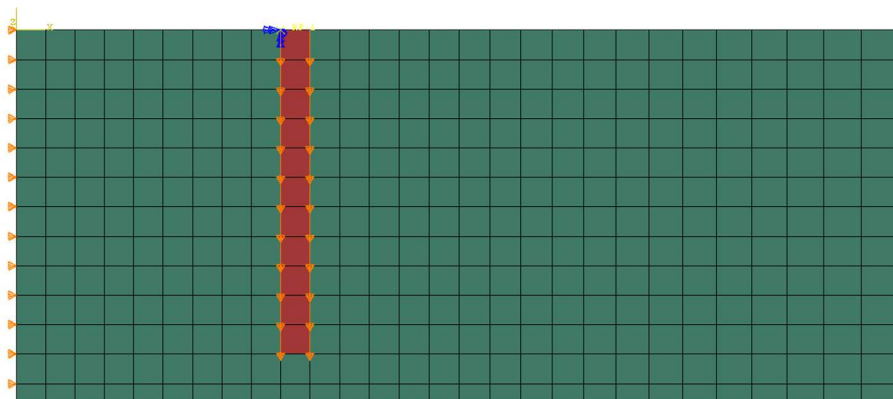


Figure 3.9 Displacement control method for static stress analysis

Finally, the methodology adopted for developing the FEM two-dimensional axisymmetric model for a rigid tubular foundation is clearly outlined in Figure 3.10.

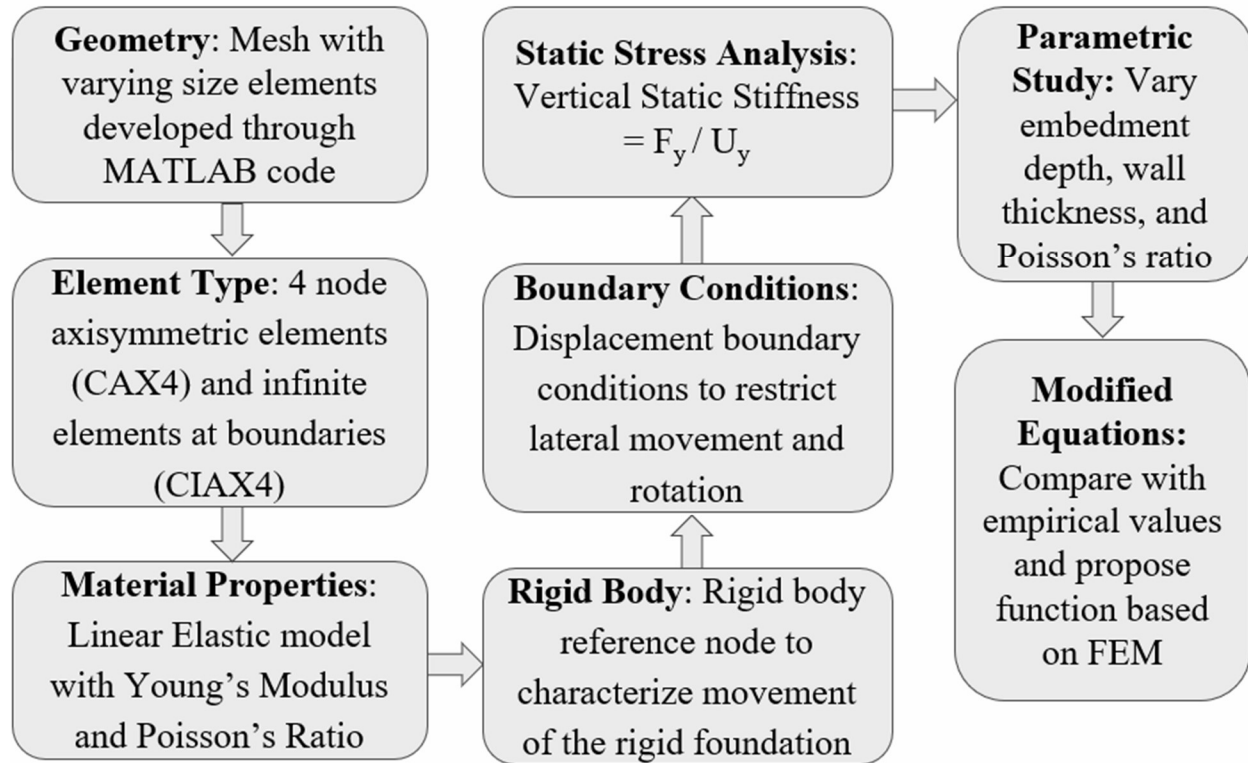


Figure 3.10 Methodology flowchart

4. RESULTS

This chapter presents the results derived from numerical modeling studies of the rigid tubular foundation. The simulations include analyzing the impact of embedment depth, wall thickness, and Poisson's ratio of soil on the foundation stiffness. This chapter begins with results of the parametric study conducted based on the parameters stated. It is followed by contours of Von Mises stress and vertical displacement of the foundation at various embedment depth and wall thickness.

4.1 Parametric Study

Stiffness is conceptually a measure of the ability of any structure to resist deformations under loads. The stiffness of an offshore wind turbine's foundation is fundamental towards deformation and natural frequency (or eigenvalue) estimations. FEM is one of the advanced methods for evaluating the foundation stiffness since it allows modeling of complex ground profiles and material models (Jalbi et al. 2017). Increase in foundation stiffness is associated with a decrease in bearing capacity. On the other hand, an increase in stiffness results in reduced ultimate settlement. It is crucial to maintain a balance between bearing capacity and settlement of an OWT's foundation. There are multiple factors which directly affect the foundation stiffness which have been explained as follows:

- **Soil Characteristics:** The type of porous media surrounding the foundation is a major contributor towards the stiffness values. For an elastic model of soil, Poisson's ratio, Young's modulus, and corresponding shear modulus of soil are major properties which must be considered for foundation design.
- **Loading Conditions:** An OWT foundation experiences a combination of loads like live loads, wind loads, seismic loads, water currents, etc. The static and dynamic stiffness of the

foundation is related to amount and pattern of loads that the structure will sustain during its service life. Figure 4.1 is a representation of loading in a sample monopile OWT foundation

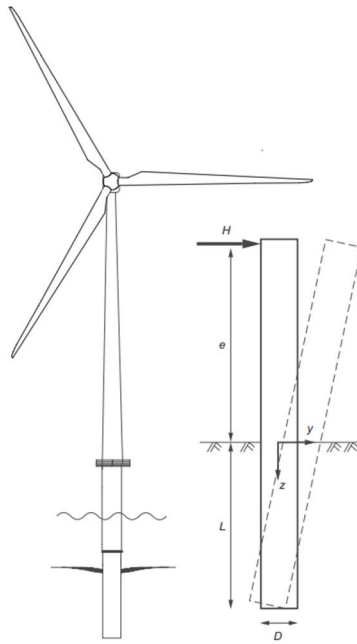


Fig. 1. A typical offshore wind turbine installed on a monopile foundation

Figure 4.1 A typical monopile foundation for offshore wind turbine. Reprinted from (Leblanc et al. 2010)

- Type of Foundation: There are several types of foundations being utilized for OWT around the world as shown in Figure 1.2. The capacity of foundations to resist loads varies with different types of foundations.
- Foundation Material: Typically, steel, or concrete material is utilized in the construction of foundations for OWTs. The material properties of foundations influence the extent of stiffness possessed by the foundation.
- Age of foundation: Strength of structures deteriorate over time due to weathering, corrosion, etc. This impacts the stiffness of foundation over its serviceable life.

The objective of this research is to focus on these parameters affecting the static vertical stiffness of a sample rigid tubular foundation embedded in an elastic half-space medium.

4.1.1 Effect of Embedment Depth

In this section, we compare the solution of Gazetas et al. 1985 and our FEM model for vertical static stiffness of a rigid tubular foundation with increasing embedment depth. Figure 4.2 summarizes the relationship between the embedment depth and embedment ratio based on the properties listed in Tables 3.1 and 3.2.

At zero embedment depth, i.e., for a surface foundation, the embedment factor for our FEM model is 3% lower than that of the empirical value given by Gazetas et al. 1985. As the depth of embedment increases and h/R becomes more than 0.3, the FEM model predicts a higher embedment factor meaning that static stiffness is much higher than it is at surface level for that specific depth. On the other hand, the principle of superposition for Gazetas et al. 1985 rigid circular foundation solution estimates a lower embedment factor beyond h/R greater than 0.3. The embedment ratio for our FEM model is 18% higher than Gazetas et al. 1985 at h/R equals to 3. On an average, the embedment factor for our FEM model is within 10% of the empirical solution for h/R from 0 to 3.

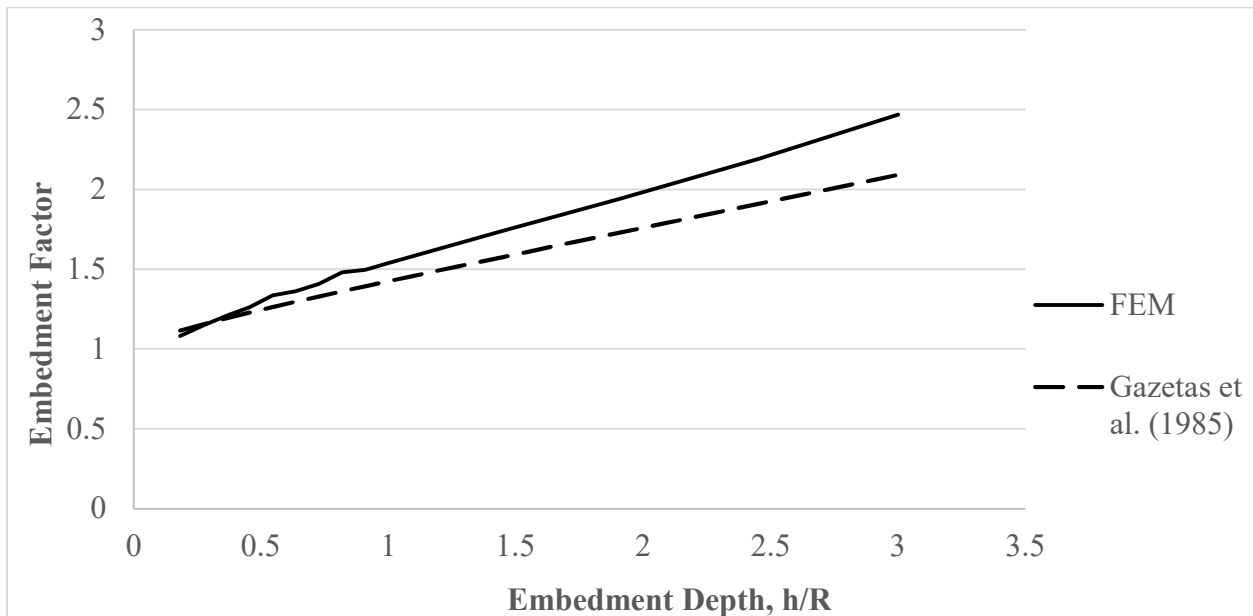


Figure 4.2 Comparative plot of embedment factor with embedment depth

4.1.2 Effect of Wall Thickness

This section reviews the impact of wall thickness of a rigid tubular foundation on its vertical static stiffness. The ratio of wall thickness of the rigid tubular foundation to that of its diameter is termed as the wall thickness factor, represented by t/D . The analysis conducted for this thesis focuses on a range of wall thickness factors from 0.05 to 0.5 where $t/D = 0.5$ refers to a rigid circular foundation (wall thickness is equivalent to the radius of foundation). The formula proposed by Aubeny 2023 is based on superposition of the elastic solution for a circular area of radius, R . It assumes a constant shape factor beyond t/D of 0.1. For wall thickness factor of less than 0.1, the FEM model static stiffness is 19% more than the empirical solution. For t/D lying within 0.1 to 0.5 range, the vertical static stiffness of the tubular foundation predicted by our representative numerical model is approximately 10% less in comparison to empirical solution.

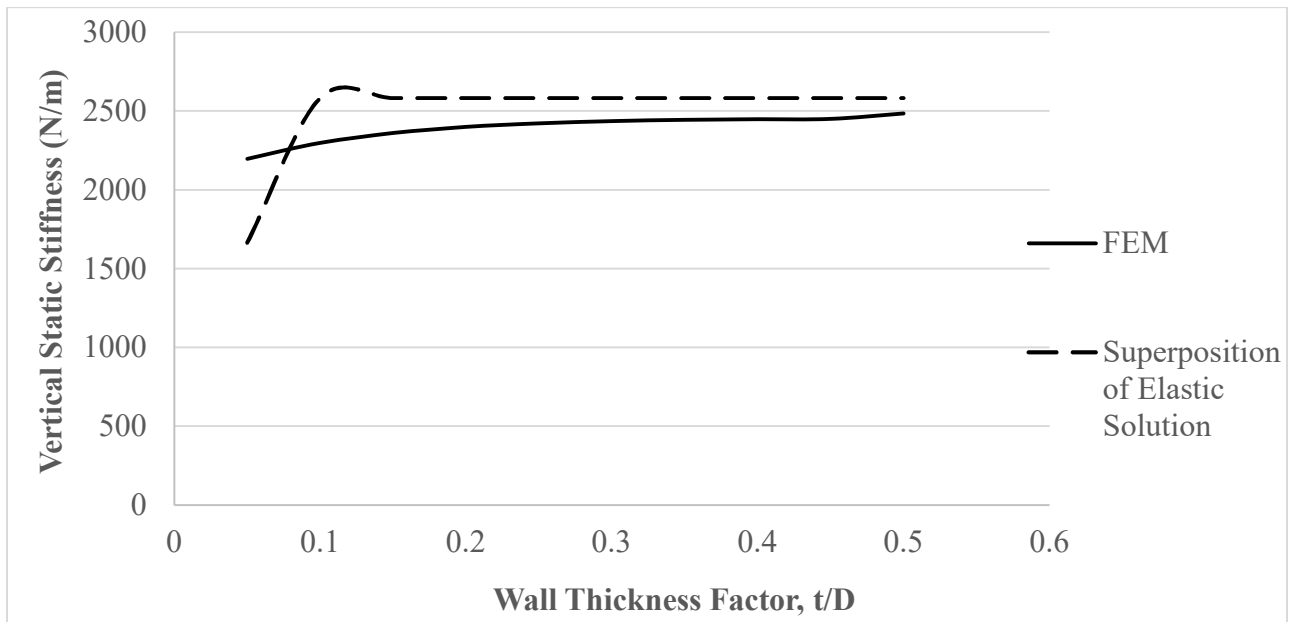


Figure 4.3 Comparative plot of vertical static stiffness with wall thickness

4.1.3 Effect of Poisson's Ratio

In this section, the wall thickness, embedment depth along with Young's Modulus is assumed to be constant to effectively analyze the impact of Poisson's ratio. The wall thickness factor, t/D is fixed at 0.05 and the foundation is assumed to be at surface. Poisson's Ratio is the ratio of transverse strain to axial strain for the same magnitude of force applied on the material. The range of Poisson's ratio ranges from 0.25 to 0.45 for our analysis which was determined by literature review of OWT foundations. A larger Poisson' ratio indicates a greater tendency of the soil to deform laterally as opposed to axial deformation. For the same magnitude of load, there will be decreased vertical settlement for a higher Poisson's ratio. Since the vertical static stiffness is inversely proportional to the vertical displacement, this results in a boosted static vertical stiffness. Figures 4.4 and 4.5 reinforce this concept with the help of our FEM model of the rigid tubular foundation.

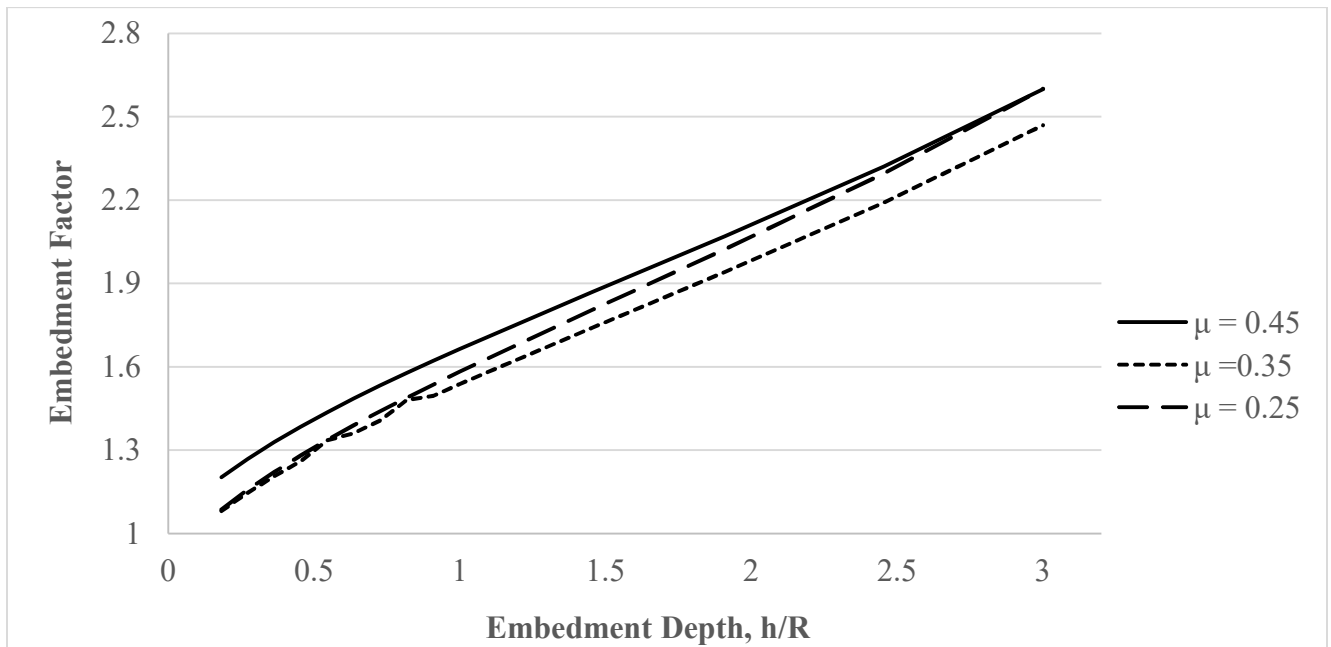


Figure 4.4 Effect of Poisson's ratio on embedment factor

In Figure 4.4, the embedment factors for Poisson's ratio 0.25 and 0.35 are within 0.05% at surface level. However, at embedment depth $h/R = 3$, the embedment factors for Poisson's ratio 0.35 and 0.45 are within 5% difference.

The increase in the wall thickness of the rigid tubular foundation leads to a greater static vertical stiffness for a larger Poisson's ratio of the soil surrounding it as shown in Figure 4.5. The vertical static stiffness FEM solution for Poisson's ratio 0.25 is 3 to 4% less than that of 0.35 Poisson's ratio. However, the vertical static stiffness FEM solution for Poisson's ratio 0.45 is approximately 7% more than that of Poisson's ratio 0.35.

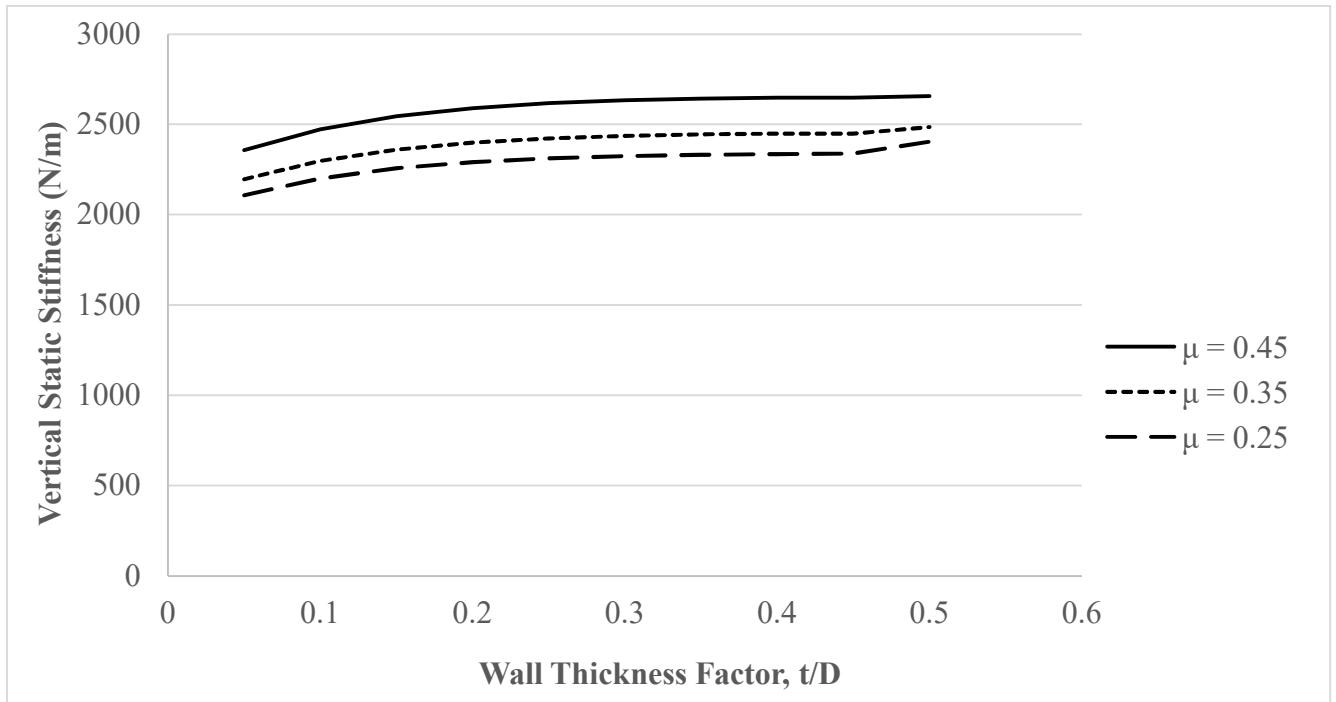


Figure 4.5 Effect of Poisson's ratio on vertical static stiffness

4.2 Stress and Displacement Contour Plots

This section provides an overview of von mises stress and vertical displacement contour plots obtained in ABAQUS for various cases utilized for our parametric study.

4.2.1 Von Mises Stress Contours

The von mises stress contour plots have been included for certain cases of embedment depth and wall thickness to understand the variation and distribution of stresses. These contour plots are highly efficient in identifying regions prone to failure with high stresses. They are instrumental towards understanding the response of the rigid tubular foundation to loading with different parameters studied in this thesis. All values of stresses are in N/m^2 .

Figures 4.6, 4.7, 4.8, and 4.9 are von mises stress contour plots for increasing embedment depth. It is evident that the region at the embedded depth beneath the foundation experiences the peak stresses. With increasing embedment depth, the overall stress experienced by surrounding soil is seen to rise.

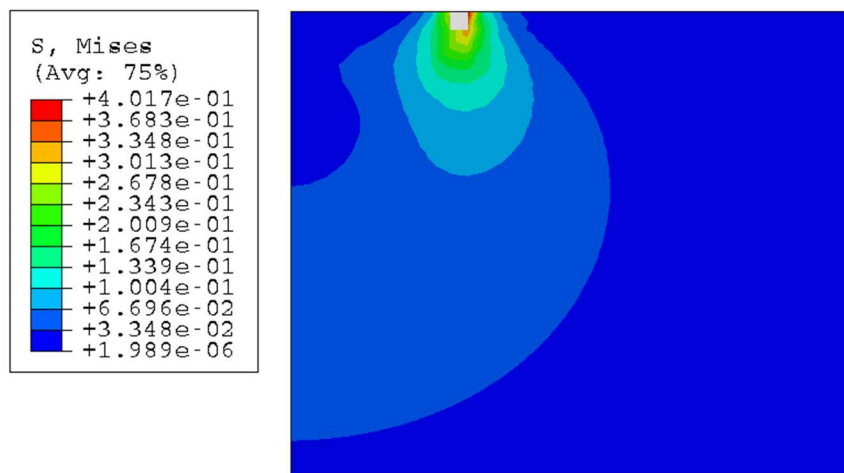


Figure 4.6 Stress contour plot for zero embedment ($h/R = 0$)

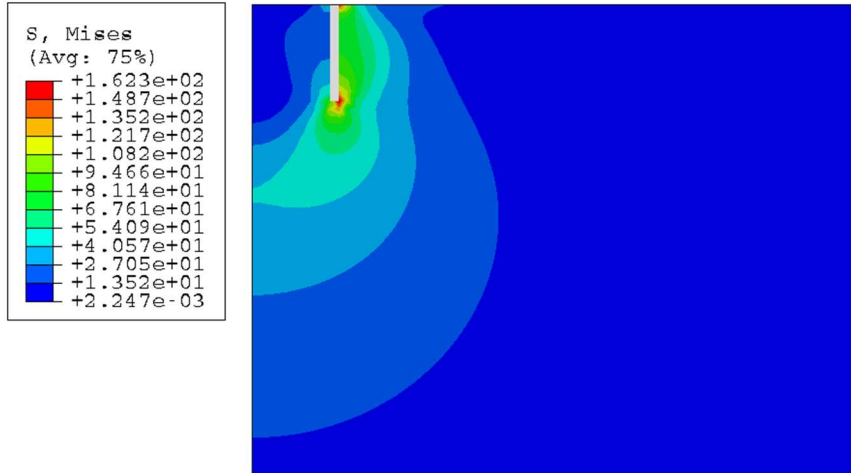


Figure 4.7 Stress contour plot for $h/R = 1$

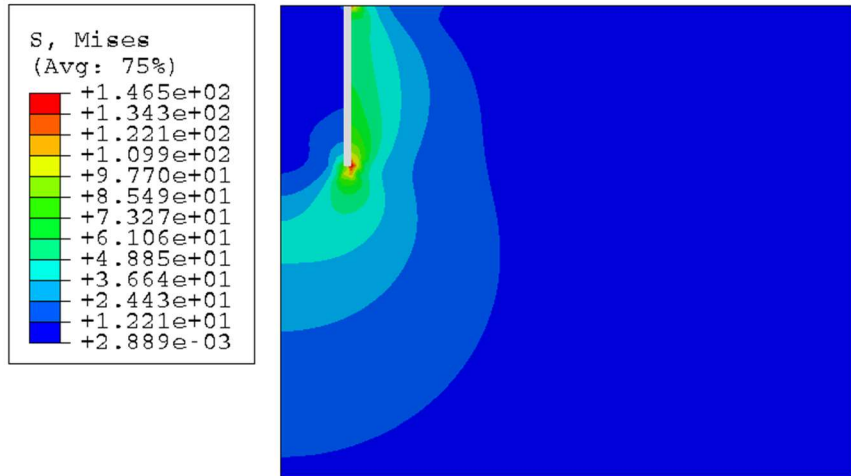


Figure 4.8 Stress contour plot for $h/R = 2$

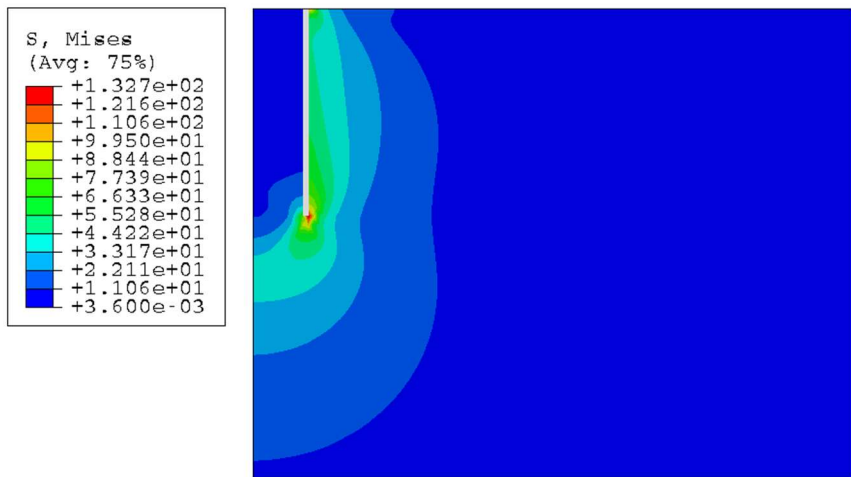


Figure 4.9 Stress contour plot for $h/R = 3$

Figures 4.11, 4.12, and 4.13 are von mises stress contour plots for wall thickness factor, t/D ranging from 0.05 to 0.5. As the wall thickness increases, the maximum stress experienced by surrounding soil increases. The maximum stresses are observed to be experienced at the edges of the rigid tubular foundation.

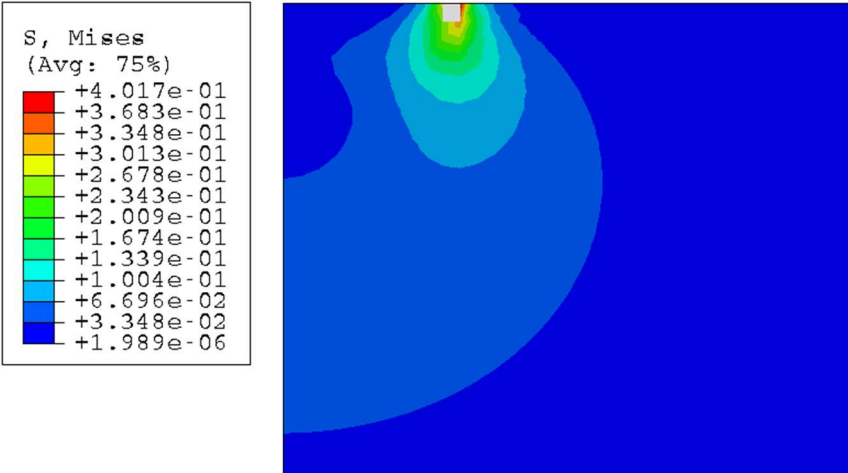


Figure 4.10 Stress contour plot for $t/D = 0.05$

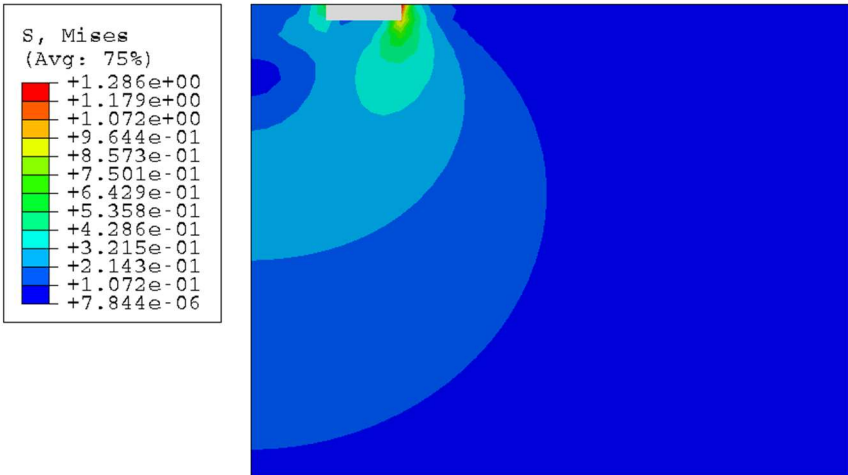


Figure 4.11 Stress contour plot for $t/D = 0.25$

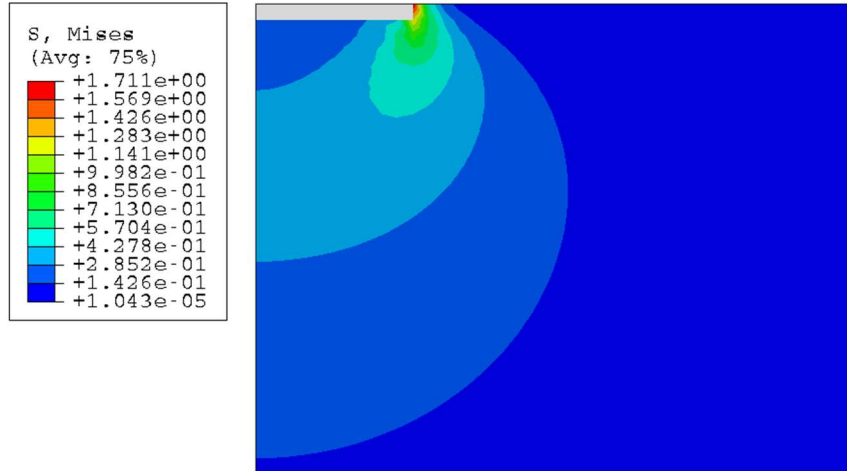


Figure 4.12 Stress contour plot for $t/D = 0.5$

4.2.2 Vertical Displacement Contours

The following contour plots are graphical representations of settlements experienced by the rigid tubular foundation with increasing embedment depth and wall thickness. All the values indicated are in meters.

Figures 4.14, 4.15, 4.16, and 4.17 are vertical displacement contour plots for increasing embedment depth. As observed, the magnitude of settlement experienced by embedded nodes increases with embedment depth.

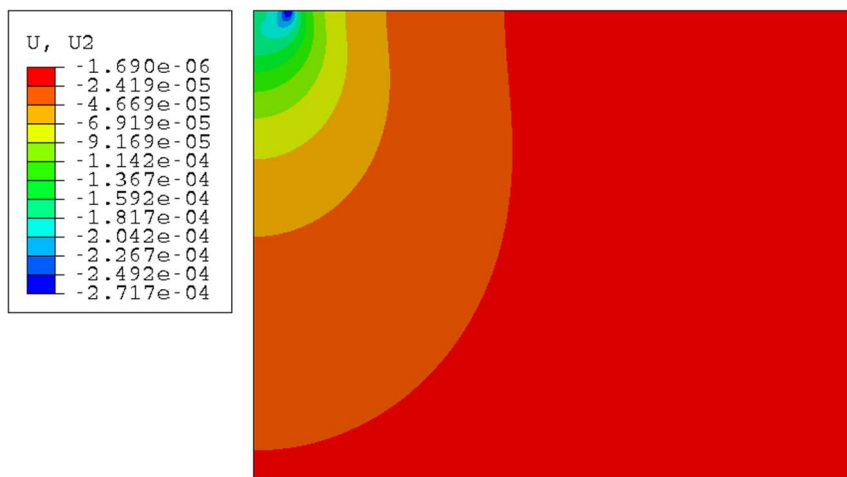


Figure 4.13 Vertical displacement contour plot for zero embedment ($h/R = 0$)

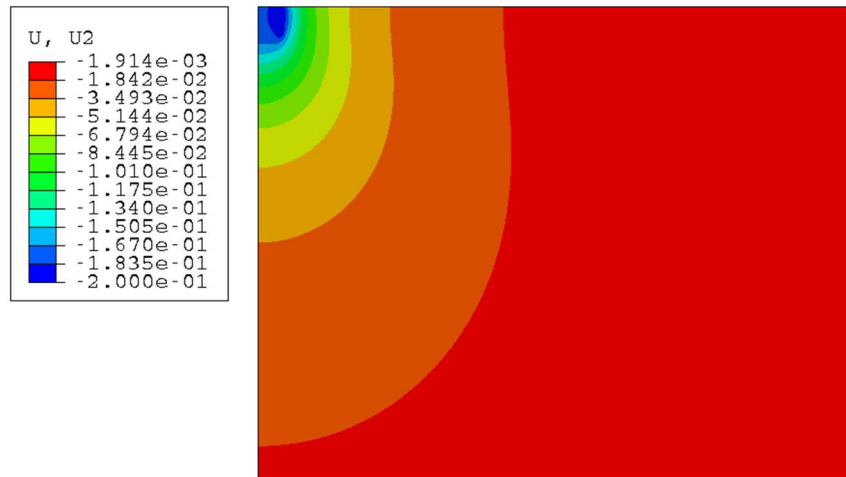


Figure 4.14 Vertical displacement contour plot for $h/R = 1$

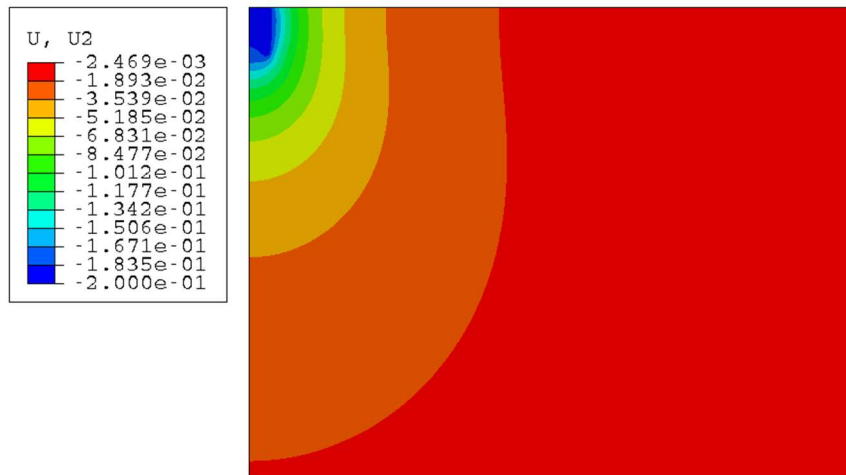


Figure 4.15 Vertical displacement contour plot for $h/R = 2$

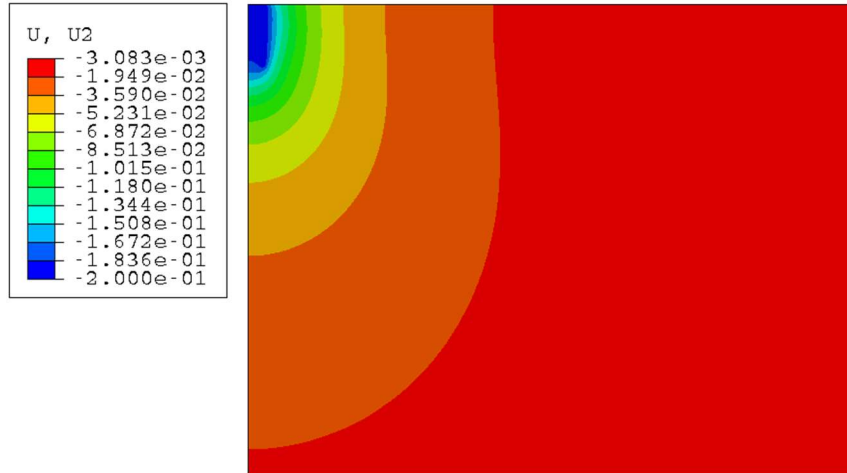


Figure 4.16 Vertical displacement contour plot for $h/R = 3$

Figures 4.18, 4.19, and 4.20 represent contour plots for settlement with increasing wall thickness factor, t/D . There is a rise in the magnitude of vertical displacement as the wall thickness increases and becomes a rigid circular footing.

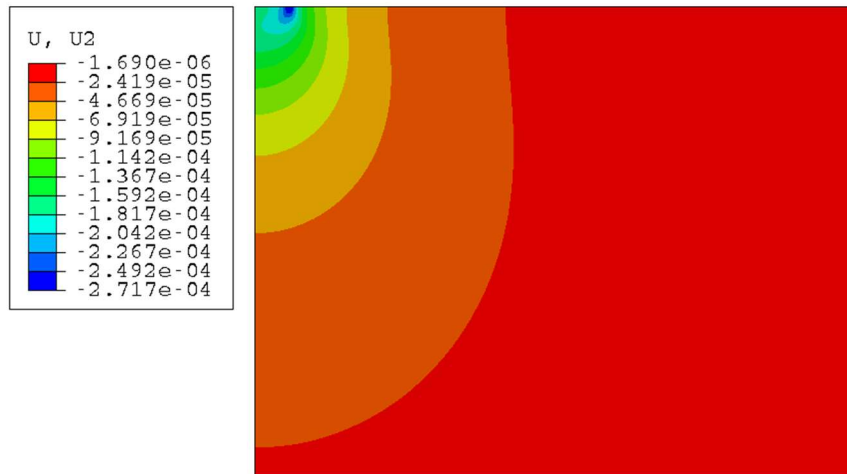


Figure 4.17 Vertical displacement contour plot for $t/D = 0.05$

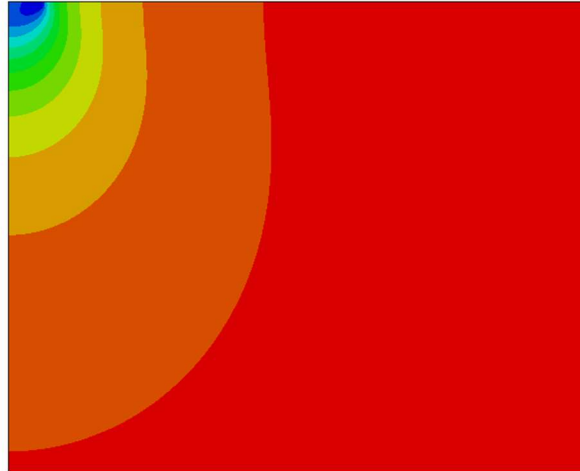
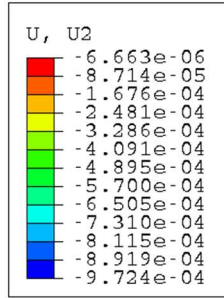


Figure 4.18 Vertical displacement contour plot for $t/D = 0.25$

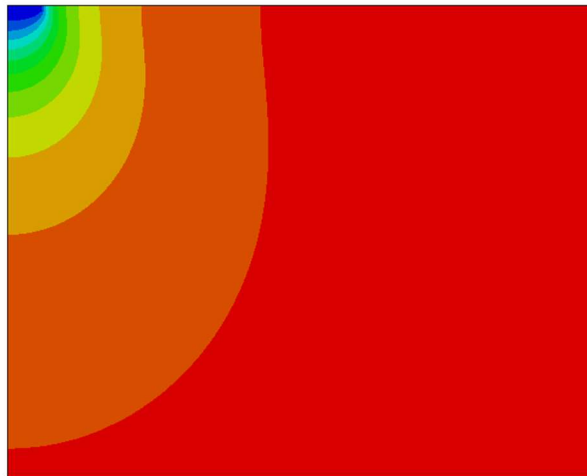
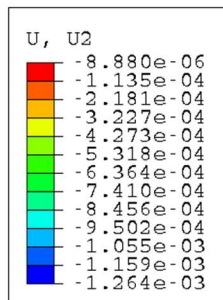


Figure 4.19 Vertical displacement contour plot for $t/D = 0.5$

5. CONCLUSIONS

Through our static stiffness analysis on an embedded bucket foundation using FEM based two-dimensional axisymmetric model, we infer the following:

1. The vertical static stiffness of a rigid tubular foundation increases with increasing embedment depth. The FEM numerical model incorporates the effect of increasing embedment depth for the rigid tubular foundation and estimates averagely 10% higher value than Gazetas et al. 1985 for embedment depth h/R more than 0.3 (meaning deeper embedment depths). Hence, we conclude that since Gazetas et al. 1985 solution is based on a surface foundation, and the empirical formulas for embedment factors may not completely capture the impact of embedment depth.
2. Gazetas et al. 1985 proposed a formula based on a rigid circular foundation. The principle of superposition for the elastic solution of a circular foundation with zero embedment (Aubeny 2023) assumes a constant vertical static stiffness beyond t/D of 0.1. For t/D of 0.5, i.e for a rigid circular foundation, the FEM numerical model solution lies within 3.7% of the elastic solution. Our model is an effort towards incorporating the effect of wall thickness on vertical static stiffness.
3. A larger Poisson' ratio of surrounding soil medium for a rigid tubular foundation signifies a greater vertical static of the foundation. The settlements caused for the same loading becomes lesser for greater Poisson's ratio.
4. The proposed equation for vertical static stiffness of an embedded rigid tubular foundation based on our FEM study is:

$$K_s = \frac{K_{s,t} \cdot K_{s,e}}{GR}$$

Here K_s = vertical static stiffness of the foundation (N/m)

$K_{s,t}$ = Vertical static stiffness as a function of wall thickness (N/m)

$K_{s,e}$ = Vertical static stiffness as a function of embedment depth (N/m)

The following polynomial equations are proposed:

$$\frac{K_{s,t}}{GR} = a (t/D)^2 + b (t/D) + c$$

$$\frac{K_{s,e}}{GR} = d (h/R)^2 + e (h/R) + f$$

Where a, b, c, d, e, and f are coefficients as given in Table below.

Table 5.1 Proposed vertical static stiffness equation constants

Poisson's ratio of soil, μ	a	b	c	d	e	f
0.25	-4.97	3.55	5.20	0.07	2.37	5.87
0.35	-5.99	4.27	5.86	0.11	2.32	6.67
0.45	-7.51	5.34	6.73	0.09	2.52	7.51

REFERENCES

- Aubeny, C. (2021, November 15). *Vibratory Installed Bucket Foundations for Fixed Foundation Offshore Wind Towers* [PowerPoint Slides]. NOWRDC Advisory Board Meeting.
- Aubeny, C. (2023). Vibratory installation of bucket foundations. *Ocean Engineering*, 273, 113895.
- Bathe, K. J. (1982). Finite element procedures for solids and structures linear analysis. *Finite Element Procedures*, 148-214.
- Boussinesq, J. (1885). *Application des potentiels à l'étude de l'équilibre et du mouvement des solides élastiques: principalement au calcul des déformations et des pressions que produisent, dans ces solides, des efforts quelconques exercés sur une petite partie de leur surface ou de leur intérieur; mémoire suivi de notes étendues sur divers points de physique mathématique et d'analyse*. Gauthier-Villars.
- Brinkgreve, R. B. (2005). Selection of soil models and parameters for geotechnical engineering application. In *Soil constitutive models: Evaluation, selection, and calibration* (pp. 69-98).
- Costoya, X., DeCastro, M., Carvalho, D., & Gómez-Gesteira, M. (2020). On the suitability of offshore wind energy resource in the United States of America for the 21st century. *Applied Energy*, 262, 114537.
- Gazetas, G., Dobry, R., & Tassoulas, J. L. (1985). Vertical response of arbitrarily shaped embedded foundations. *Journal of geotechnical engineering*, 111(6), 750-771.

- Girjavallabhan, C. V., & Reese, L. C. (1968). Finite-element method for problems in soil mechanics. *Journal of the Soil Mechanics and Foundations Division*, 94(2), 473-496.
- Guo, Y., Wang, H., & Lian, J. (2022). Review of integrated installation technologies for offshore wind turbines: Current progress and future development trends. *Energy Conversion and Management*, 255, 115319.
- Jalbi, S., Shadlou, M., & Bhattacharya, S. (2017). Practical method to estimate foundation stiffness for design of offshore wind turbines. In *Wind Energy Engineering* (pp. 329-352). Academic Press.
- Kausel, E., & Roesset, J. M. (1975). Dynamic stiffness of circular foundations. *Journal of the Engineering Mechanics Division*, 101(6), 771-785.
- Kausel, E., & Ushijima, R. (1979). Vertical and torsional stiffness of cylindrical footings. *Research Rep*, 76, 6.
- Leblanc, C., Byrne, B. W., & Houlsby, G. T. (2010). Response of stiff piles to random two-way lateral loading. *Géotechnique*, 60(9), 715-721.
- Lepert, P., Briaud, J. L., & MAXWELL, J. (1991). Dynamic Method to Assess the Stiffness of Soil Underlying Spread Foundations. *Integrity Testing of*, 199, 1.
- McKenna, R., Pfenninger, S., Heinrichs, H., Schmidt, J., Staffell, I., Bauer, C., ... & Wohland, J. (2022). High-resolution large-scale onshore wind energy assessments: A review of potential definitions, methodologies and future research needs. *Renewable Energy*, 182, 659-684.
- O'Kelly, B. C., & Arshad, M. (2016). Offshore wind turbine foundations—analysis and design. In *Offshore Wind Farms* (pp. 589-610). Woodhead Publishing.)

Poulos, H. G., & Davis, E. H. (1974, August). Elastic solutions for soil and rock mechanics. Textbook. Figs, Tabls, Refs: John Wiley and Sons Inc. 1974, 411P. In *International Journal of Rock Mechanics and Mining Sciences & Geomechanics Abstracts* (Vol. 11, No. 8, p. A159). Pergamon.

Sánchez, S., López-Gutiérrez, J. S., Negro, V., & Esteban, M. D. (2019). Foundations in offshore wind farms: Evolution, characteristics and range of use. Analysis of main dimensional parameters in monopile foundations. *Journal of Marine Science and Engineering*, 7(12), 441.

Selvadurai, A. P. (2013). *Elastic analysis of soil-foundation interaction*. Elsevier.

Skopljak, N. (2016, March 31). *EEW SPC Rolls Out World's Heaviest Monopile*. Offshore Wind. <https://www.offshorewind.biz/2016/03/03/eew-spc-rolls-out-worlds-heaviest-monopile/>.

Sture, S. (2004). *Determination of Soil Stiffness Parameters* [PowerPoint Slides]. Short Course on Computational Geotechnics & Dynamics, University of Boulder, Colorado. <https://ceae.colorado.edu/~sture/plaxis/slides/>

Wu, X., Hu, Y., Li, Y., Yang, J., Duan, L., Wang, T., ... & Liao, S. (2019). Foundations of offshore wind turbines: A review. *Renewable and Sustainable Energy Reviews*, 104, 379-393.